

ELECTROHYDRODYNAMIC INSTABILITY IN A MICROCHANNEL UNDER AN
AC FIELD

by

Berkay Keklik

B.S., Chemical Engineering, Ege University, 2016

Submitted to the Institute for Graduate Studies in
Science and Engineering in partial fulfillment of
the requirements for the degree of
Master of Science

Graduate Program in Chemical Engineering
Boğaziçi University
2018

to the people who cared about me

ACKNOWLEDGEMENTS

In this Master of Science journey of many challenges, I am grateful for the people supporting me in different ways. To start with, I would like to express my truthful gratitude to my thesis supervisor Assoc. Prof. Abdullah Kerem Uğuz for his guidance, indulgence and trust in me. He gave me a vision on not only research but also on life that I will always benefit. It was a privilege for me to work with him during this study.

I would also like to express my sincere appreciations for the members of the thesis committee, Assist. Prof. Hilal Taymaz Nikerel and Prof. Ramazan Yıldırım for reading and commenting on my thesis.

Additionally, I would like to thank Sercan Altundemir, Seymen İlke Kaykanat, Suat Canberk Ozan and Pınar Eribol for their considerable time and effort in my research. The time I have shared with them will be remembered. I should especially thank Mustafa Olcay Türkmen for his effort and concern in my research. Even though he was in another research group and had no benefit on helping me, he accompanied me on my experiments. I am also grateful to Sevgi Sena Macit for the motivational support and assistance in this research.

This journey is not only completed by running the experiments. For that matter, I thank Ahmet Coşgun for all the tobacco support he provided throughout this research and Ezgi Öztürk for helping me find my path. I am thankful to Merve Yüce for always having extra tea for all the researchers in Department of Chemical Engineering. Also I would like to express my gratitude to Müge Kasım for the partnership in Advanced Fluid Mechanics course which boosted my interest in fluid mechanics.

Apart from the research, I thank my dear friends Sinan Cem Deveci, Özgün Özkul, Canan Uçar, Şükran Şençekiçer from The Atatürk Institute for Modern Turkish History and Beşir Özgür Nayır from the Philosophy Department for contributing my life in the campus intellectually. Thanks to them, my time in Boğaziçi University wasn't always about engineering.

Finally, I would like to express my dearest appreciations to all my family members for their patience, encouragement and moral support throughout my whole education.

Boğaziçi University Research Fund Grant Number 14000 and TÜBİTAK Project 116M374 are acknowledged for the financial support.

ABSTRACT

ELECTROHYDRODYNAMIC INSTABILITY IN A MICROCHANNEL UNDER AN AC FIELD

In this study, the electrohydrodynamic instability between two immiscible liquids for two different liquid couples, Newtonian/Newtonian and non-Newtonian/Newtonian is experimentally studied. The liquid couples are pumped into a rectangular cross-section microchannel with electrodes on the side walls. An alternating current (AC) electric field is applied with sinusoidal or square waves. As Newtonian liquids, silicone oils with different viscosities, ethylene glycol and 85% glycerol-water solution are used. For the non-Newtonian liquid, 250 ppm xanthan gum is dissolved in 85% glycerol solution. At a certain voltage, called the hitting voltage, the interface that formed between the two immiscible liquids flowing in the microchannel loses its flat form and hits the channel walls. The hitting voltage value for various thickness ratios, total flow rates and AC field frequencies are investigated. The instability provides microdroplets if the applied voltage is approximately $200 V_{pp}$ more than the hitting voltage. Increasing the thickness ratio, defined as the thickness of the dispersed phase to that of the continuous phase, has an increasing effect on the hitting voltage for both liquid couples. The total flow rate has also an increasing effect on the hitting voltage but the effect is more significant for the non-Newtonian/Newtonian liquid couple than the non-Newtonian/Newtonian liquid couple. The AC field frequency shows a jump for the hitting voltage at some critical frequency. The applied function type has a significant effect on the hitting voltage. It is observed that the hitting voltages for the square function are not only lower than the sinusoidal values, but also has a linear whilst sinusoidal has an exponential trend. Particle encapsulation experiments are also performed and it is seen that encapsulating particles is possible but controlling it requires very high precision tools.

ÖZET

BİR MİKROKANALDA AC ELEKTRİK ALANI ETKİSİNDE ELEKTROHİDRODİNAMİK KARARSIZLIK

Bu çalışmada, alternatif akımlı (AC) elektrik alana tabi tutulmuş, biri Newtonyen/Newtonyen, diğeri Newtonyen olmayan/Newtonyen olmak üzere iki farklı sıvı çifti kullanılarak iki karışmayan sıvı arasındaki elektrohidrokinamik kararsızlık incelenmiştir. Sıvı çiftleri, yan duvarlarında elektrotlar bulunan dikdörtgen bir mikrok kanalın içine pompalanmıştır. Elektrotlardan alternatif akımlı elektrik alan, sinüsoidal ve kare dalgalar halinde uygulanmıştır. Newtonyen sıvılar olarak farklı viskozitelerde silikon yağları, etilen glikol ve %85 gliserol-su çözeltisi kullanılmıştır. Newtonyen olmayan sıvı için de %85 gliserol çözeltisi içerisinde 250 ppm ksantan gum çözülmüştür. İki karışmayan sıvı arasındaki arayüzey, düzgün formunu kaybederek duvara çarpmaktadır. Buna sebep olan gerilime, çarpma gerilimi denmektedir. Çarpma gerilimi, farklı kalınlık oranları, toplam debiler ve AC elektrik alan frekansları için incelenmiştir. Kararsızlıklar, çarpma voltajının yaklaşık olarak 200 Vpp üzeri uygulanırsa eğer, mikro damlacık oluşumu sağlayabilmektedir. Dağınık fazın sürekli faza olan kalınlık oranını arttırmak, iki sıvı çifti için de çarpma voltajını arttıran etkiye sahiptir. Toplam debiyi arttırmak da benzer şekilde çarpma voltajını arttıran etkiye sahiptir. Toplam debinin çarpma voltajına olan etkisi Newtonyen olmayan/Newtonyen sıvı çifti için Newtonyen/Newtonyen sıvı çiftine göre daha belirgindir. Uygulanan AC elektrik alanını etkisi ise sadece belirli bir frekansta görülmektedir. İşbu frekansı geçince çarpma voltajı birden artmakta ancak tekrar sabitlenmektedir. AC elektrik alanının fonksiyon tipi de kayda değer bir etkiye sahiptir. Sonuçlara göre kare fonksiyon uygulandığında elde edilen çarpma voltajı trendleri hem sinüsoidal olanlardan daha düşük hem de lineer bir trende sahiptir. Sinüsoidal fonksiyonda ise trend üstel özelliktedir. Damlacık içerisine parçacık hapsedme deneyleri de yapılmış ve bunun mümkün olduğu görülmüştür. Ancak kontrollü şekilde yapılabilmesi için hassasiyeti yüksek ekipmanlar gerekmektedir.

TABLE OF CONTENTS

ACKNOWLEDGEMENTS	iv
ABSTRACT	vi
ÖZET	vii
LIST OF FIGURES	ix
LIST OF TABLES	xii
1.INTRODUCTION	1
2. LITERATURE SURVEY	3
2.1. Microchannel Fabrication	3
2.2. Application of Droplet Microfluidics	4
2.3. Droplet Generation Methods	5
2.4. Electrohydrodynamic Instabilities	6
2.5. Alternating Current (AC) Electric Field	9
2.6. Non-Newtonian Liquids in Microfluidics	11
3. EXPERIMENTAL WORK	13
3.1. Chemicals	13
3.2 Experimental Set-up	13
3.2.1. Design of the Microchannel	16
3.2.2. Fabrication of the Microchannel	16
3.3. Procedure of the Experiments	20
4. RESULTS AND DISCUSSION	23
4.1. Determining the Hitting Voltage	25
4.1.1. The Effect of the Thickness Ratio	25
4.1.2. The Effect of the AC Electric Field Wave Form	31
4.1.3. The Effect of the Frequency of the AC Electric Field	32
4.2.1. Applications	34
4.2.1. Particle Encapsulation	34
4.2.2. Generating Two Droplets with Different Sizes	36
5. CONCLUSION	37
REFERENCES	38
APPENDIX A: INTERFACE POSITION	44

LIST OF FIGURES

Figure 1.1.	(a) Two-fluid flow instabilities under the effect of the electric field (b) Schematic of the phenomenon and the coordinate systems (Haiwang et al., 2012)	2
Figure 3.1.	Experimental set-up syringe pump (1), microscope (2), microchannel (3), function generator (4), oscilloscope (5), amplifier (6), high speed camera (7), computer (8).	14
Figure 3.2.	The syringes to the microchannel connection. a) The tubes connected to the syringes. b) The tubes connected to the microchannel.....	15
Figure 3.3.	AC electric field system. Oscilloscope, Function Generator and Amplifier	15
Figure 3.4.	Schematic of a microchannel	16
Figure 3.5.	Laser cut PMMA sheets with the dimensions of 50 x 25 x 3 mm	17
Figure 3.6.	Cut acetate sheets	18
Figure 3.7.	Taped acetate sheets	18
Figure 3.8.	Last form of the acetate sheets	19
Figure 3.9.	Final form of the microchannel.....	19
Figure 3.10.	Top view from an experiment. A Stable flat interface between two immiscible liquids	22
Figure 4.1.	The mechanism of the hitting of the interface on the wall a) A stable interface at 800 Vpp b) The interface at 900 Vpp c) The interface at 1100 Vpp d) The interface at 1190 Vpp.....	24

Figure 4.2.	The first droplet formation for 100 $\mu\text{L}/\text{min}$ and 200 $\mu\text{L}/\text{min}$ for the silicone oil and 85% glycerol solution at 1400 Vpp.....	25
Figure 4.3.	Theoretical and experimental thickness ratios comparison of the silicone oil 10 cSt and the 85% glycerol solution	27
Figure 4.4.	The hitting voltage of the Newtonian liquid couple for different thickness ratios and total flow rates of 300, 240, 180 $\mu\text{L}/\text{min}$ (TF).	28
Figure 4.5.	Rheology of 250 ppm 85% Glycerol Solution.	29
Figure 4.6.	The hitting voltage of the Newtonian & non-Newtonian liquid couple for different thickness ratios and total flow rates of 300, 240, 180 $\mu\text{L}/\text{min}$	30
Figure 4.7.	Comparison of the hitting voltage for the Newtonian and the Newtonian/non-Newtonian liquid couple at the flow rate of 300 $\mu\text{L}/\text{min}$...	31
Figure 4.8.	Comparison of the hitting voltages of the silicone oil 50 cSt and ethylene glycol liquid couple with the electric fields of sinusoidal and square waves at the total flow rate of 350 $\mu\text{L}/\text{min}$	32
Figure 4.9.	Frequency dependency of the hitting voltage at the sinusoidal and square electric field with the silicone oil 10 cSt and ethylene glycol liquid couple at the total flow rate of 350 $\mu\text{L}/\text{min}$	33
Figure 4.10.	Initial interface deflection at particle encapsulation experiments with the flow rates of 20 $\mu\text{L}/\text{min}$ 50 cSt silicone oil and 50 $\mu\text{L}/\text{min}$ ethylene glycol a) Particle at stable interface at the silicone oil side b) First hit of the interface to the wall at 2500 Vpp	35

Figure 4.11.	Particle encapsulation with the flow rates of 50 $\mu\text{L}/\text{min}$ 50 cSt silicone oil and 20 $\mu\text{L}/\text{min}$ ethylene glycol a) First encapsulation in 2500 Vpp b) The slug form after the first encapsulation.....	35
Figure 4.12.	Droplet generation with the flow rates of 100 $\mu\text{L}/\text{min}$ 50 cSt silicone oil and 500 $\mu\text{L}/\text{min}$ ethylene glycol a) Stable interface b) Small droplet generated with directly applied 1300 Vpp at 0.33 Hz c) Big droplet's head d) Big droplet's back.....	36
Figure A.1.	Physical system of the microchannel	44

LIST OF TABLES

Table 3.1.	The chemicals used in the experiments.....	13
Table 4.1.	Error percentage of the thickness ratios of the silicone oil 10 cSt and ethylene glycol liquid couple in Figure 4.3.....	26
Table 4.2.	Rheological data on the non-Newtonian liquid at 23°C.....	30

1. INTRODUCTION

Microfluidics is a science and technology that investigates and develops devices working in the micro scale which can pump, manipulate, monitor and control small volumes of fluids. Microfluidics offer several useful capabilities: usage of very small quantities of samples, low cost and short time analysis, carrying out high resolution and sensitivity separations.

There are various applications of microfluidics. Some of them are inkjet printers, blood analyzers, drug administering, gradients generation, cell analysis, lab-on-a-chip systems and micro analysis systems. Aside from the diagnostics, biotechnology, environmental technology and pharmaceuticals, microfluidics has also proven success in consumer electronics, photolithography, paper chemical and food industries (Anthonysamy, 2007).

One research area of microfluidics is droplet-based microfluidics. Contrary to continuous flow systems, droplet-based systems aims to create diverse volumes with utilization of immiscible phases. Microfluidic systems have low Reynolds number ($Re \ll 1$) which dictates laminar flow regime. Droplet microfluidics offers to perform reactions without increasing the device complexity or size and involves manipulation and generation of droplets inside micro devices. Independent control of droplets can be achieved, it generates individually transported, mixed and analyzed micro reactors. Therefore parallel experimentation can be performed (Sharma *et al.*, 2013).

There are active and passive methods to generate droplets. Passive methods can be categorized as breakup in co-flowing streams, T-junctions and flow focusing. More recently, emerging technologies introduced actively generating droplets by electric field (Zhu *et al.*, 2016).

In breakup in co-flowing streams, dispersed phase is driven into the continuous phase by a small inner channel. The droplets break up from an extended liquid jet and droplet is generated at the tip of the inner channel.

T-junction method is a configuration that involves the dispersed phase perpendicularly intersects the main channel which contains the continuous phase. The interface is formed at the junction point. The shear forces generated by the continuous phase and the subsequent pressure gradient cause the head of the dispersed phase to elongate into the main channel until the neck of the dispersed phase thins and eventually breaks.

In flow focusing, the dispersed and continuous phases are forced through a narrow region in the device. The aim is to create a singular point of highest shear. And the highest shear point exists at the narrowest region of a nozzle. The break-off of droplets occurs consistently at that point thus uniform droplets are formed (Teh *et al.*, 2008).

Creating droplets by electrohydrodynamics is done by applying an electric field to a Poiseuille flow of two immiscible fluids. Electric field changes the interface stress balance between the fluids. To apply an electric field, the device is embedded with electrodes. After a critical voltage, the interface hits to the wall of the channels and droplets form. Figure 1 presents a possible configuration.

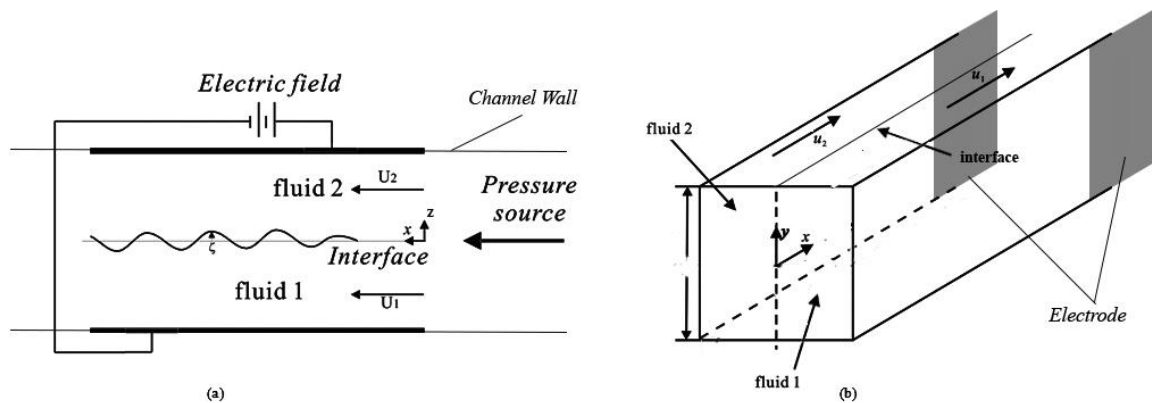


Figure 1.1. (a) Two-fluid flow instabilities under the effect of the electric field (b) Schematic of the phenomenon and the coordinate systems (Haiwang *et al.*, 2012)

2. LITERATURE SURVEY

In this chapter, microchannel fabrication methods are reviewed and applications of droplet microfluidics are explained. Then the droplet generation methods which can be categorized as active and passive, are presented. In active methods, application of the alternating current (AC) electric field method to grow the instabilities on the interface then generating droplets is the main subject of this thesis. Therefore electrohydrodynamics and researches on AC are introduced. Lastly, non-Newtonian liquid studies in microchannels are reviewed.

2.1. Microchannel Fabrication

Microchannel fabrication is a challenging part of microfluidic science. Working at micro scale dictates nearly-perfect channel structures to minimize uncontrolled disturbance effects on the experiments.

First fabrication is made by Terry *et al.* (1979) by micromachining inspired from semiconductor and microelectronic industry. At first, glass is used for the channels, which is understandable considering durability, compatibility and light transmittance; but, the fabrication cost of glass channels is high compared to other materials (Fiorini and Chiu, 2005). Hence, plastic materials are generally used in the fabrication processes.

Roberts and Kumar (2010) used a laser machine to a part of the thermoplastic channel material. With heat, the material is engraved. Laser beam is directed to the part that is desired to be removed from the channel. The laser-touched areas are melted due to the thermoplastic characteristic of the material.

Xia and Whitesides (1998), introduced soft lithography technique. It is a low-cost method for the fabrication of microchannels. The method is built around replica molding and self-assembly. In this process, to generate patterns, an elastomeric stamp is used. The surface of this stamp has a patterned relieved structures on it. With this method, polydimethylsiloxane (PDMS) can be used as the material of the channels.

2.2. Application of Droplet Microfluidics

Droplet formation in microfluidics is a promising research area due to the many advantages that include but not limited to using small samples in both industrial and laboratory applications. With micro droplets, it is possible to work at molecular scale, cells or reactors by using very small volumes and observing them in isolated and controlled droplets.

Using micro droplets for chemical purposes is reasonable to minimize the cost and working safely due to the fact that chemical reagents being expensive and dangerous. In biochemical applications, small volumes and short time may be required to perform analyses, detections and multiple reactions are preferred. These requests can be satisfied by using micro droplets which serve as micro reactors. For example, in micro droplet reactors, nanoparticles or organic molecules (Hatakeyema *et al.*, 2006) can be synthesized. Capability of adjusting the reagent composition and good mixing, provided enhanced size distribution and the yield. The emulsion polymerase chain reaction (PCR) is a successful biological method and applied commercially. The use of the droplets prevent the interaction between the channel walls with DNA templates and polymerases. Consequently, the contamination of the sample caused by the interaction is prevented (de Mello, 2001).

Another application of droplet microfluidics is seen in the area of protein crystallization, which is used to study a protein structure by X-ray crystallography. Proteins start to form crystals when the solution becomes superheated. Due to the problem of protein sample sources being limited, the amount of samples should be reduced to the range of 4 nL to 10 μ L for the experiments, which can be achieved by utilizing nanoliter-sized droplets (Song *et al.*, 2006; Zheng *et al.*, 2004). Small sample volumes do not always indicate dilution. After storing a single cell in a droplet, an increase in the density occurs due to the confinement of the single cell. Therefore, the molecules are released, which provides less time required to detect the released molecules by the cell (Song *et al.*, 2006).

2.3. Droplet Generation Methods

As mentioned previously, there are two main methods of droplet generation, i.e., passive and active methods. In the passive methods, the channel geometry is used to generate droplets. Some of the passive methods are T-shaped junctions (Thorsen *et al.*, 2001), co-flowing streams (Umbanhowar *et al.*, 2000), and flow focusing devices (Anna *et al.*, 2003). In passive methods, only flow rate manipulation can be used to control the droplet size.

Droplets can also be generated by active methods. The advantage of the active methods is, having at least one more parameter that can be controlled in addition to the flow rates of the liquids. With this advantage, both the droplet generation frequency and the droplet size can be controlled.

There are several active methods to generate droplets. Some of them are making use of thermal effects, pressure, electric and magnetic field.

Thermal effects generate droplets by using the temperature dependency of the interfacial tension between the liquid couple and their viscosity. A stable liquid couple at a certain temperature may be unstable at another temperature value. Changing the temperature creates instability therefore droplets are generated. Nguyen *et al.* (2007) studied this effect and changed the temperature between 25 to 70°C. Study showed that increasing the temperature has an increasing effect on the droplet size and that dependency fits on an exponential curve.

Murshed *et al.* (2008) studied the temperature effect on droplet size in a PDMS T-junction microchannel. They also demonstrated that droplet size is directly affected and proportional to temperature. In addition, they found that temperature effect on droplet size is greater in smaller microchannel depths.

Tan *et al.* (2008) generated droplets in a flow focusing device with an integrated micro heater. Experiments started with the dripping regime of the flow focusing device at room temperature. Then, the temperature was increased and above 30°C, droplets were formed in

other regimes of the flow focusing device. Therefore, they concluded that temperature has a regime changing effect in flow focusing devices.

Changing the flow pressure can be used to manipulate droplets. Willaime *et al.* (2006) performed experiments in a T-junction microchannel configuration with a membrane integrated to the secondary actuation channel. The secondary actuation channel is filled with water and the pressure is changed; therefore, the membrane is deflected and this deflection affected the flow velocity of the dispersed phase which increased the droplet generation frequency.

Another study of pressure effect is studied in a flow focusing device. Chen *et al.* (2006a; 2006b) worked in a device with pressure chambers on the both sides of the flow focusing orifice. To apply pressure, a pressurized gas is used. Applying high pressure to the orifice creates greater instability and generates smaller droplets with increased generation frequency.

Magnetic field is also a tool to manipulate droplet generation. Manipulation and generation of ferrofluid droplets with magnetic field in a T-junction microchannel is investigated by Tan *et al.* (2010). It is observed that droplet sizes change with the magnetic field strength. They studied the generation from the absence to the presence of the magnetic field and found that magnetic field strength has an increasing effect on the droplet size.

2.4. Electrohydrodynamic Instabilities

Melcher *et al.* (1968) investigated dynamical effects of charge relaxation on electromechanical surface waves propagation on the lines of an electric field. The study indicates that the charge relaxation provides overstability to liquid-liquid or liquid-gas interfaces. Results show, in the limit of zero conductivity, an applied tangential electric field on the interface between dielectric fluids stabilizes the surface perturbations. The model predicts two mechanisms to induce an overstability. The first method is the polarization surface forces normal to the peak deflection regions. The regions are shifting in temporal phase by the relaxation of free charge. The second is free charges relaxing the interface act as a negative viscosity (Melcher *et al.*, 1968).

Schaffer *et al.* (2001) performed experiments and developed a model to study the effect of electric fields on viscous polymer fluids in thin film geometry. They obtained different stages of instabilities due to the applied electric field charge and annealing time. They claimed that they can collapse their data on a master curve that can be described by the model.

Ozen *et al.* (2006) investigated the electrodynamic instability between two immiscible liquids to form monodisperse droplets in a square channel. They aimed to control the droplet size and formation rate by controlling the amplitude of the electric field and the flow rates of the liquids. Their technique provided control of the droplet size within about 1%. They observed the destabilization effect of the electric field on the liquid-liquid interface for different voltage values. The results show that as the voltage difference increases, the droplet size decreases, and also the droplet size and frequency remain constant over time for constant voltage difference and flow rate.

Uguz *et al.* (2008) performed a linear stability analysis of a flat interface between two leaky dielectric fluids for fast electrical relaxation times. They formulated the linear stability analysis of a two-fluid layer flowing in a channel that is subjected to an electric field. They found that the electric field destabilization effect is broader for a normal electric field than a parallel field and that they both have stabilizing effect for certain conductivity and electrical permittivity combinations.

Roberts *et al.* (2010) used linear stability analysis to investigate the effect of free charge and alternative current electric fields on the stability of immiscible trilayer systems. It is shown that AC electric have similar effect on both perfect dielectric bilayers and trilayers. The accumulating charge at the air/liquid interface is leading to a faster growth rate. They demonstrated that AC electric field can be used control the accumulating charges at top and bottom interfaces and also that with an AC electric field it is possible to generate smaller diameter pillars than the DC electric field.

Li *et al.* (2012) studied analytically and experimentally electrohydrodynamic instability of the interface between two immiscible fluids. The two-layer system is subjected

to a normal electric field. They observed that the applied voltage has a destabilizing effect while the viscosity, flow rates and electrical mobility of the fluids have a stabilizing effect.

Nam *et al.* (2012) studied a simple and label free method for separating micro particles using the elasto-inertial characteristic of a non-Newtonian fluid in a microchannel. At the inlet, by introducing sheath fluid from the center, they pushed the particle containing flow towards the side walls. Particles with 1-5 μm diameter that were suspended in viscoelastic fluid are separated in the outlet channels. They noticed that while the larger particles are gathered on the centerline of the outlet, the smaller particles are flung towards the side walls with minimal lateral migration. Results showed that different sized particles can be sorted with an efficiency of more than 99%. They also demonstrated that this method can be applied for blood separation with extremely high purity in continuous flow.

Eribol and Uguz (2015) studied the electrohydrodynamic instability between two immiscible liquids and the effect of various parameters on the interfacial instability. Electric field is applied in a microchannel with electrodes that has two immiscible fluids inside which are pumped by a syringe pump. The studied parameters are the ratios of viscosities, the width of channel, the flow rates and the direction of electrical field (parallel or normal to the flat interface between the immiscible liquids). Altundemir *et al.* (2018) performed experiments to investigate the droplet formation mechanism in a microchannel subjected to DC electric field. They used ethylene glycol and silicone oil with various viscosities. They analyzed the effect of the viscosity, the thickness ratios and the total flow rate of the liquids on the critical voltage where the interface starts to deflect. The results show that the viscosity and the thickness ratios have an increasing effect on the critical voltage; however, the total flow rate has no effect on it.

Wang and Papageorgiou *et al.* (2018) investigated axisymmetric deformation and the stability of two immiscible viscous, leaky dielectric liquids in an annulus between two cylinders in the presence of an electric field, which is provided by applying constant voltage between the cylinders. They derived equations for the interface of the inner and outer liquids in the limit of long wave. First, they solved the system without an electric field and it is found that the interface non-linearly evolves in the direction of both the vicinity of the inner and the outer electrodes and the interface touches the closest wall. When the electric field is

applied, the interface may touch either wall depending on the conductivity ratio. When the conductivity ratio of the outer liquid to the inner liquid is very small, the interface touches the inner wall. And if the conductivity ratio is large, the interface touches the outer wall.

2.5. Alternating Current (AC) Electric Field

AC electric field is one of the parameters that controls the droplet formation mechanism and its size. Castro-Hernandez *et al.* (2017) used an AC electro flow-focusing device under moderate voltages (500-700 V peak-to-peak) to produce droplet groups. Due to the Hagen-Poiseuille flow in the microchannel, smaller droplets moved faster than the larger droplets. And it is seen that the droplet generation frequency is twice of the signal frequency. Huang *et al.* (2018) investigated AC electric field effect on the droplet control in flow focusing microchannel with a Newtonian and a non-Newtonian fluid. First, they produced droplets with flow-focusing, and then they applied an AC electric field on the droplets. It is observed that the AC electric field induced Maxwell stress and it stimulates interfacial instability leading to smaller size of droplets. It is seen that frequency has an effect on the storage and loss modulus of the non-Newtonian fluid. With increasing frequency, both storage and loss modulus increase but with a different rate. In low frequencies, storage modulus is smaller than loss modulus but after a certain value, storage modulus exceeds loss modulus.

Soni *et al.* (2018) performed an experimental research with AC electric field and compound droplets. They used 0.1M NaCl/castor oil for compound droplet and silicone oil as the continuous phase. They observed two independent parameter effects; the ratio of the core radius to shell radius and the frequency of the AC electric field. They demonstrated that with an increase of the frequency and the radius ratio, the relative phase difference decreases.

Sarang and Reza (2017) performed simulations to overcome the low Reynolds number inside the microchannel with AC electric field provided by the electrodes embedded at the channel walls. The particles inside the novel twisted microchannel with four semi-circular obstacles to observe velocity distribution inside the channel. The chaos effect was increased by utilizing the Coanda effect. It was demonstrated that the mixing efficiency in water increased with increasing applied voltage. With the combination of time-dependent electric

field and initial pumped flow, they were able to drive an AC electrokinetic (ACEK) flow. The AC electro-osmosis (ACEO) force and Coanda effect provided chaos regime inside the microchannel.

Roberts and Kumar (2009) made theoretical studies on AC electrohydrodynamic instabilities in thin films. They used linear stability analysis for perfect and Floquet theory for leaky dielectric models. Linear stability analysis shows that the use of an AC field slows growth rate compared to DC electric field. Frequency of the AC electric field also has a strong effect on the interfacial charges, therefore the growth rate. They demonstrated that higher frequencies cause a decrease in the growth rate. Roberts and Kumar (2010) also investigated another study on the effect of the AC field and the free charge on trilayer films by using linear stability analysis. For perfect dielectric films, they considered the equivalent DC field to compare with the AC field and for the leaky dielectric films, has different pillar configurations from perfect dielectric films. For that reason, they claim that AC field can be utilized for specifying the location of free charge in the trilayer system. Results show that AC electric fields have a similar effect on perfect dielectric trilayer with perfect dielectric bilayers which is the fastest growth rate and wavenumber provided by lower frequency values.

Espin *et al.* (2013) studied AC and DC field caused instabilities in viscoelastic thin films. Perfect and leaky dielectric materials subjected to AC and DC fields are considered. For DC field, asymptotic analysis and for AC field Floquet theory are employed. It is found that elasticity increases the maximum growth rate and the wave number that corresponds to it. In leaky dielectric models, charge accumulate at the interface which leads to faster growth rates and single instability mode.

Paul *et al.* (2017) performed experiments to understand deformation and electrohydrodynamic motion of the droplets under AC electric field application. Silicone oil and water droplets are suspended in castor oil medium. It is seen that both silicone oil and water droplets are deformed to a prolate shape under AC electric field which was fixed to 50 Hz. The terminal velocity was also dropped by increasing the electric field strength.

2.6. Non-Newtonian Liquids in Microfluidics

Wong *et al.* (2017) simulated droplet formation in two phase flow with a Newtonian and a non-Newtonian fluid in a T-junction microchannel. The Sodium Carboxymethylcellulose (SCMC) concentration in the non-Newtonian fluid gives the shear-thinning nature. They empirically observed that rheological and physical properties of the fluids obey Carreau-Yasuda stress model. The strongest effects on the droplet size caused from the Newtonian continuous phase and the flow rate. According to their results, increasing the flow rate decreases the droplet size and the dispersed phase rheology has a smaller effect. Droplet diameter generally gets smaller with an increase in SCMC concentration and they believe that this is due to the viscosity ratio change.

Roumpea *et al.* (2017) experimentally investigated the plug flow of a non-Newtonian and a Newtonian fluid in a quartz microchannel. They used two-color particle image velocimetry to obtain the hydrodynamic characteristics and velocity profiles under different flow rates. The experiments showed that the concentration increase of the non-Newtonian fluid, produces longer, bullet-shaped plugs and increases the thickness of the surrounding film. It is observed that the addition of the non-Newtonian fluid extended the area of the plug flow to higher superficial phase velocities compared to the Newtonian fluid addition. Plug lengths, front plug edge curvature, the thickness of the aqueous film between the plug and the channel wall are increased with the increased concentration of the non-Newtonian fluid. And the velocity profile measurements showed that the addition of the non-Newtonian fluid results higher plug velocity also.

Kunti *et al.* (2017) made numerical investigations for the characterization of non-Newtonian fluids on the efficiency of mixing in an alternating current (AC) electrothermal micromixer which was fed by electrothermal pump. Results show that shear dependent viscosity of the non-Newtonian fluid has a strong effect on the mixing quality. Higher flow does not allow the fluids to mix under consideration of residence time and flow highly depends on flow behavior index. Pseudoplastic fluids prevent vortices in the channel, causing a poorer mixing quality and conversely dilatant fluids almost always provides perfect mixing at the outlet of the channel. When it comes to AC potential, mixing quality increases up to a certain critical voltage and then falls gradually.

Ren (2018) modeled alternating current (AC) electrothermal mechanism for efficient pumping of blood flow in a microfluidic device by using hybrid boundary element method (BEM) and immersed boundary-lattice Boltzmann method with the Carreau-Yasuda model. As parameters, voltage magnitudes and frequency of the AC, electrode configurations, the channel length, channel height and thermal boundary conditions of electrodes are investigated. He demonstrated that the frequency-dependent dielectrics of the blood makes it different from common Newtonian aqueous solutions. Thermally insulated electrodes could increase the efficiency of the pumping significantly and increasing the voltage is more economical than adding extra electrodes to the channel with the same energy consumption.

Raj M *et al.* (2018) have fabricated polydimethylsiloxane microfluidic phantoms to study the fluid-structure interaction which is caused by the interaction between a deformable wall and a non-Newtonian fluid. A shear-thinning xanthan gum solution is used as the non-Newtonian fluid. They analyzed the microfluidic phantom steady flow characteristics by deformation, pressure drop and flow visualization using micro-PIV. They developed a model for the deformation under pressure driven flow. Deformation on the wall was small compared to the channel diameter but they believe these results will have a contribution in the design of polymeric microfluidic phantoms.

Li and Xuan *et al.* (2018) performed experiments to analyze fluid rheology effect on the particle migration in a rectangular microchannel. They examined both Newtonian and non-Newtonian shear-thinning fluids to see the behavior difference between them. And the results indicated that the fluid elasticity caused the particles to move towards the center and the shear thinning property caused them to both move towards the center and the corners.

3. EXPERIMENTAL WORK

In this section, the used chemicals, the experimental set-up, the microchannel fabrication, and the procedure of the experiments are explained.

3.1. Chemicals

The chemicals that are used in the experiments are shown in Table 3.1

Table 3.1. The chemicals used in the experiments

Chemicals	Formula	Source
Ethylene Glycol	$C_2H_6O_2$	Merck
Silicone Oil 10 cSt	$Si(CH_3)_2O)_x[Si(CH_3)(C_6H_5)O]_y$	Brookfield
Silicone Oil 50 cSt	$Si(CH_3)_2O)_x[Si(CH_3)(C_6H_5)O]_y$	Brookfield
Glycerine 85%	$C_3H_8O_3$	Isolab
180-212um PE Microspheres	$(C_2H_4)_n$	Cospheric
Xantham Gum	$C_{13}H_{10}O$	Tekkim

3.2. Experimental Set-up

In this section, the experimental set-up is shown and explained with the structure of the microchannel. Figure 3.1 shows the experimental set-up which consists of a syringe pump, a microscope, a microchannel, a function generator, an oscilloscope, an amplifier, a high speed camera and a computer.

The liquids are sent to the microchannel by a twin syringe pump (Harvard Apparatus Pump 33, Holliston, MA) and two plastic syringes (Set Medical Inc, Istanbul, Turkey) with 19.13 mm diameter. Butterfly catheter infusion sets (Harvard Apparatus Standard Butterfly Catheter Infusion Sets, Holliston, MA) with a diameter of 0.81 mm are connected to the syringes and the poly ethylene micro medical tubes (Scientific Commodities INC, Lake Havasu City, Arizona) with 1.22 mm outer and 0.72 mm inner diameter by the opposite points of the catheter. Then the other point of the tubes are connected to the microchannel. Hence, the connection from the pumps to the microchannel is provided successfully with no leakage (Figure 3.2.).

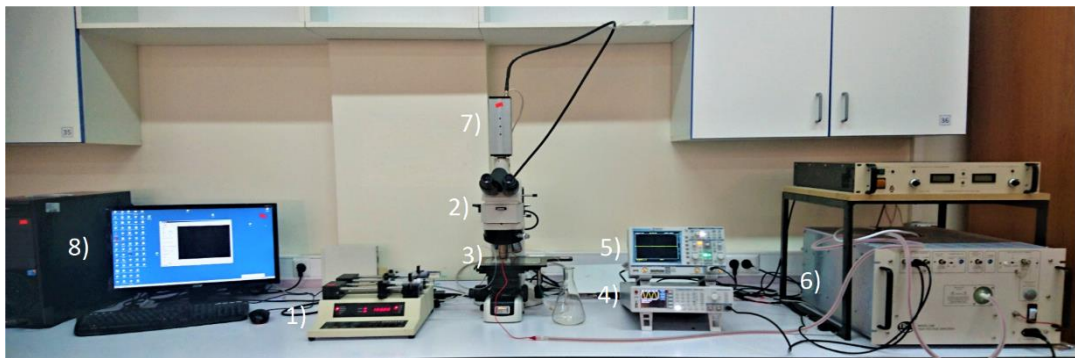


Figure 3.1. Experimental set-up syringe pump (1), microscope (2), microchannel (3), function generator (4), oscilloscope (5), amplifier (6), high speed camera (7), computer (8).

To apply an electric field, three devices are connected to each other and then to the electrodes of the microchannel as in Figure 3.3. An arbitrary waveform generator (Rohde & Schwarz HMF2525, Munich, Germany) is used to specify the form of the electric field waves and an oscilloscope (Rohde & Schwarz HMO1002, Munich, Germany) is used to observe the electric field waves. Then, the arbitrary waveform generator connected to the amplifier (Trek Inc 5/80, Lockport, NY) and the voltage that is applied by the arbitrary waveform generator is multiplied by 1000. Then the crocodile of the amplifier is attached to one of the electrodes of the microchannel and the ground electric crocodile to the other electrode. In Figure 3.3, the AC field system is shown.

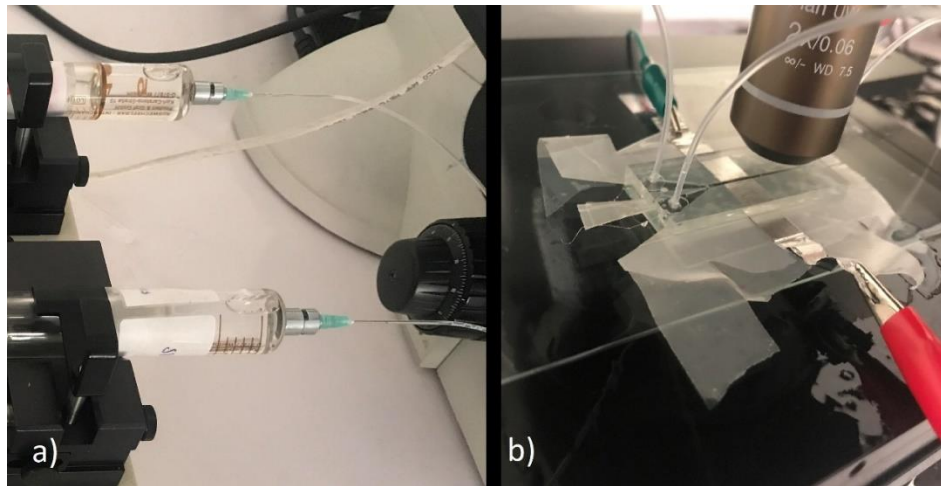


Figure 3.2. The syringes to the microchannel connection. a) The tubes connected to the syringes. b) The tubes connected to the microchannel

Nikon Eclipse LV100POL Microscope with a 2x objective is used for visualization of the experiments. The images are recorded up to 60 fps with Fastec InLine High Speed Camera which is plugged on top of the microscope and also connected to the computer. The videos and images are recorded with the software FIMS 3.0.5 and then played with QuickTime Player.

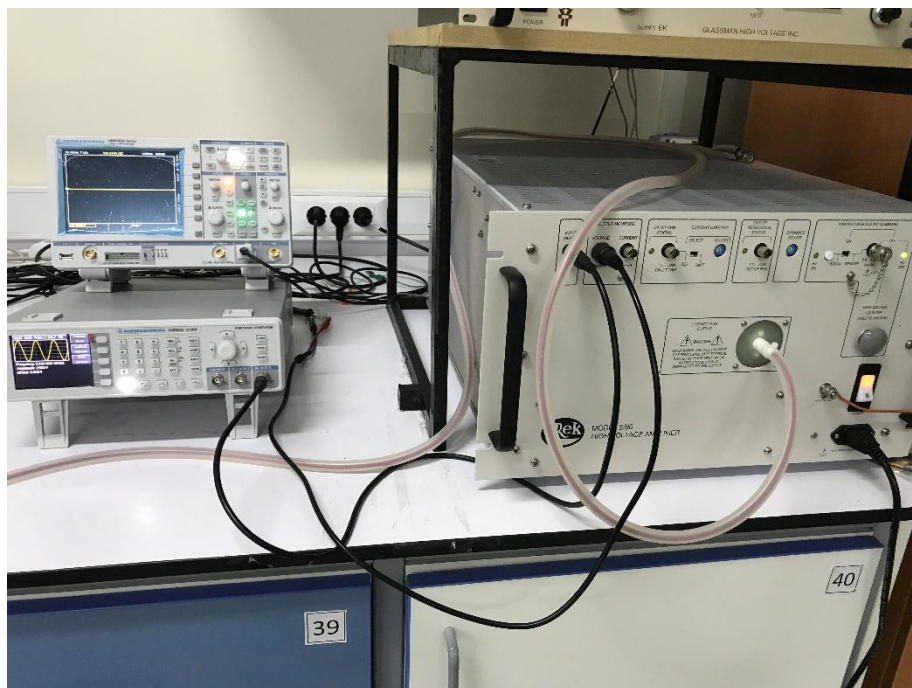


Figure 3.3. AC electric field system. Oscilloscope, Function Generator and Amplifier

3.2.1. Design of the Microchannel

The microchannel is designed with a rectangular cross section and an electric field is applied in the direction normal to the flat interface between the two immiscible liquids. The electrodes are planned to oppose each other at the sides of the microchannel walls as shown in Figure 3.4. The flow should be fully developed between the electrodes so that flat interface assumption can be made. To provide a fully developed flow and a stable interface, an entering zone is required. A length around 1 mm is required before reaching the electrodes after the y-shaped inlet.

Another zone at the outlet is necessary for the interface to prevent the end effect which is caused by the motion of the liquids leaving the microchannel.

Except the electrode zone, all of the other zones are fabricated by non-conductive materials to isolate the electric field in a specific region. For the electrode zone, conductive tape is used.

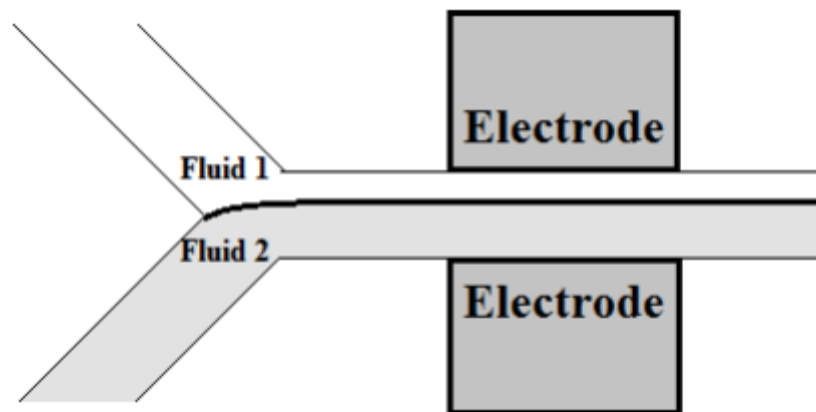


Figure 3.4. Schematic of a microchannel

3.2.2. Fabrication of the Microchannel

The fabrication materials are PMMA sheets with a thickness of 3mm (Koluman Plastik, Turkey), invisible tape (MAS, Turkey), conductive tape (Akbant, Turkey), and acetate sheet (Bilgi Dağıtım Kitap, Kırtasiye ve Büro Malzemeleri Tic. Ltd., Turkey).

For the top and the bottom layer of the microchannel, the PMMA sheets of 50 mm long, 25 mm wide, and 3 mm thickness are cut by laser. Then, to be able to attach the tubing to the microchannel, holes are opened and the final form is shown in Figure 3.5. Another plate with same sizes without holes is also required for the bottom.



Figure 3.5. Laser cut PMMA sheets with the dimensions of 50 x 25 x 3 mm

The acetate sheets of 50 mm long, 30 mm width and 0.25 mm thickness are cut (Figure 3.6). The width should be larger than the width of the PMMA chips so that an extra zone is obtained at the left and right exterior surfaces of the microchannel. This zone will be used to attach the crocodiles from the amplifier to the channel.

The sheets are covered with one-sided tapes and alumina tapes. Alumina tapes are utilized as electrodes. The entrance and the exit of the microchannel should be free of electric field so that the one-sided tapes are used in those regions. The electrode length is 1 cm, the entrance and the exit length are approximately 1 and 1.5 cm respectively. The aim of using one-sided tape is to provide flat wall on the sides due to the thickness of the one-sided tape

being the same with the alumina tape, so that the flat interface can be obtained. The electrode regions are aligned so that the electric field can be applied normal to the interface between the two liquids. Side surfaces of these sheets are planned to be the walls of the microchannel as in Figure 3.7.



Figure 3.6. Cut acetate sheets



Figure 3.7. Taped acetate sheets

Double-sided tapes are used to adhere the acetate sheets to the PMMA sheets. To form the entrance, a piece that has right angle triangle form are cut from the acetate sheets. Another triangle form acetate sheet is cut to divide the entrance flows from each other. This piece is also covered with one-sided and double-sided tapes to obtain a piece that has the same thickness with the rest of the channel walls (Figure 3.8).

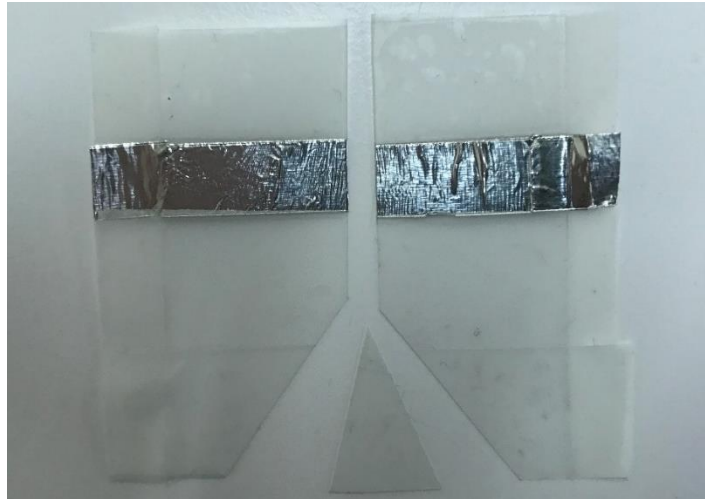


Figure 3.8 Last form of the acetate sheets

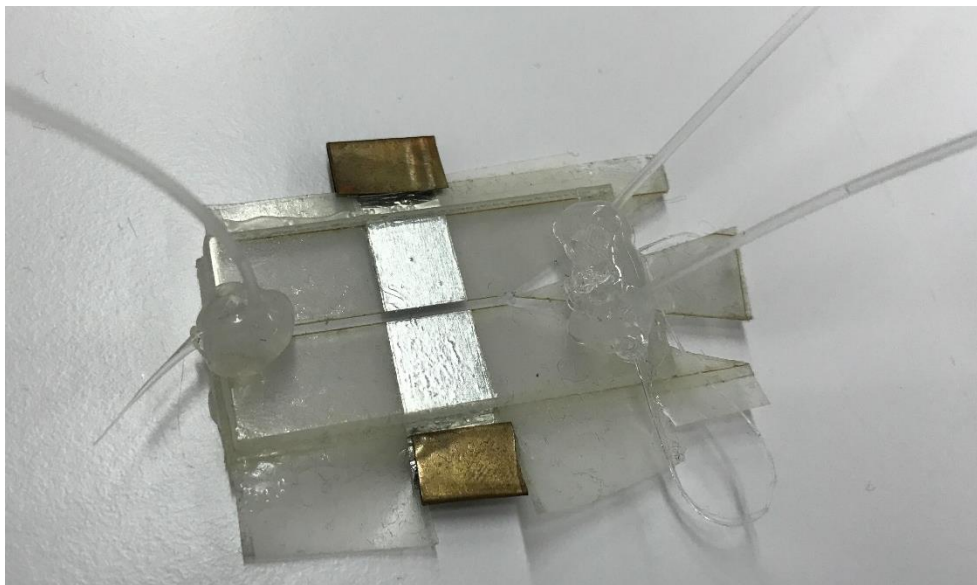


Figure 3.9 Final form of the microchannel

Finally, all of the pieces are adhered together. The holes on the microchannels being the inlet and outlet streams with attached tubing. The outer sides of the microchannel is also adhered to prevent the leakages from the entrance and the exit. Figure 3.9 shows the final form.

To perform the experiment, the microchannel put on the microscope and the crocodiles are attached to the electrodes.

Final sizes are:

Electrode length: 1 cm

Width: 1.1 mm

Depth: 0.5 mm

3.3. Procedure of the Experiments

- When the experimental setup is ready to perform the experiments, syringe pump is used to provide the desired flow rates. Both liquids are simultaneously pumped into the microchannel through polyethylene (PE) tubing. When they meet in the microchannel, they form a flat interface (Figure 3.10).
- Once a stable position is obtained, the position of the interface is recorded. Then, the function generator, the oscilloscope, and the amplifier are turned on. The minimum voltage that can be applied is 10 V; therefore, the experiment is started by applying 10 V. The applied voltage is increased gradually (with 10 V_{pp} steps) using the increasing button of the function generator.
- If the interface starts to deflect, the waiting time between the increasing steps is extended and the voltage is continued to increase after the interface is restabilized at a point. The interface is restabilized with a different form. It has a crest that does not move. It maintains that shape unless the voltage is increased as in Figure 4.1.

- At a certain voltage, the interface hits the wall and that voltage is recorded. This point is called the hitting voltage. When the interface hits the wall, that shape does not change.
- In order to obtain droplets, the applied voltage should be increased by an average of $200 V_{pp}$. Note that this is peak to peak voltage.
- When the required data is recorded, the applied voltage is decreased and set to the minimum value of $10 V_{pp}$ again. At this point, the amplifier is turned off.
- The interface restabilization at the initial position can be handled in two ways. First way is to wait but this takes a long time. Therefore, increasing the total flow rate and setting the thickness ratio to 1 and setting it to the initial values again provides faster restabilization.
- For the experiments of spherical polyethylene particles with 150-180 μm diameter mixed with 50 cSt silicon oil, the dispersion is vibrated before putting it on to the syringe pump to provide a nice homogenous dispersion.
- Electric field is applied when the particles started to be seen in between the electrodes and then are encapsulated in the droplets.
- To verify the hitting voltage, each experiment is performed at least 3 times and the average is recorded.

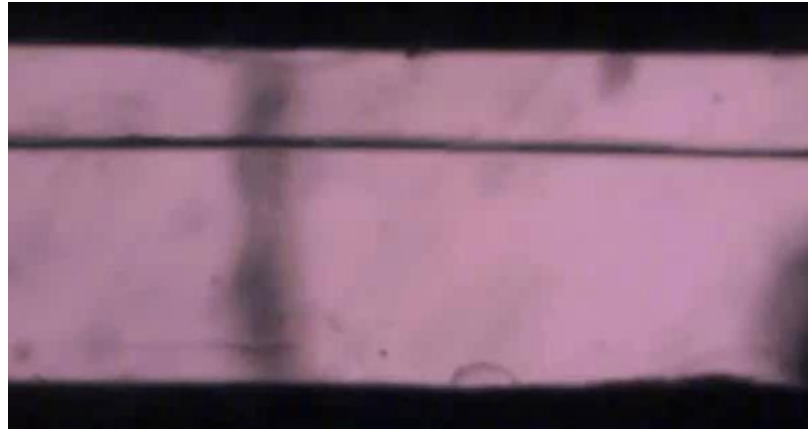


Figure 3.10. Top view from an experiment. A Stable flat interface between two immiscible liquids

4. RESULTS AND DISCUSSION

In this section, the effect of various parameters on the AC field voltage required for the interface between the two immiscible liquids to hit one of the walls, i.e. the hitting voltage is investigated and discussed. The parameters are:

- (i) The thickness ratio, β , which is the ratio of the thickness of the dispersed phase (oil) to the continuous phase (aqueous).
- (ii) The rheology of the continuous phase, which is non-Newtonian shear-thinning.
- (iii) The total flow rate, Q which is the sum of the flow rates of the dispersed and the continuous phases.
- (iv) The frequency of the electric field.
- (v) The function of the AC current, i.e., sinusoidal or square.

In all experiments, the dispersed phase is 10 or 50 cSt silicone oil and the continuous phase is either ethylene glycol or 85% glycerol solution or 250 ppm xanthan gum in %85 glycerol solution.

In Figure 4.1 the hitting characteristic of the interface under an AC electric field effect is shown when an alternating current (AC) electric field is applied. The interface between the two immiscible liquids starts to bend and a peak occurs towards the end of the electrodes. When the applied voltage reaches the hitting voltage, this peak of the interface hits the wall that is on the side of the dispersed phase and this process may provide controlled micro droplet formation depending on the applied voltage. According to Altundemir et al. (2017) results, DC electric field experiments show a different mechanism. In those experiments, when a DC field is applied, the interface has a flat form and that form does not change until a specific voltage is reached. They call this specific voltage as critical voltage.

To perform the experiments, first, a flat interface is obtained and then using the function generator and the amplifier, an electric field is created and is applied in a direction normal to the interface. The applied voltage is observed on the oscilloscope. The hitting voltage is investigated by performing a parametric analysis. All voltages are reported as peak to peak value.

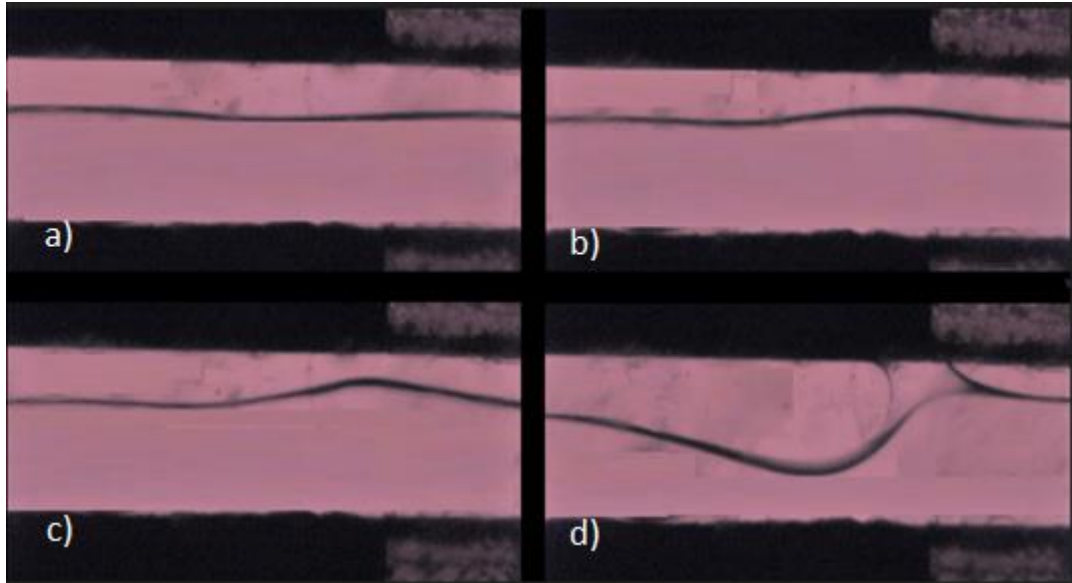


Figure 4.1. The mechanism of the hitting of the interface on the wall a) A stable interface at $800 V_{pp}$ b) The interface at $900 V_{pp}$ c) The interface at $1100 V_{pp}$ d) The interface at $1190 V_{pp}$

The liquid couple in Figure 4.1 is silicone oil 10cSt at the top and 85% glycerol solution at the bottom. The perspective of these images is the top view; hence, the liquids flow side by side. The flow rates are $100 \mu\text{L}/\text{min}$ and $200 \mu\text{L}/\text{min}$ for the silicone oil and 85% glycerol solution, respectively. The flow rates correspond to a ratio of 0.5 and the thickness ratio, β is 3.5. In the figure, the voltage of the electric field is gradually increased starting from 0 V for which the interface is flat. Once a critical voltage is reached, which cannot be easily determined as the interface oscillates with very small amplitudes, the interface starts to bend and form a crest. The crest becomes pointier as the voltage is increased further. At $800 V_{pp}$ (Fig 4.1a), the interface is still stable. At $900 V_{pp}$ (Fig. 4.1b), the disturbance on the interface grows and the interface starts bending. At $1100 V_{pp}$ (Fig. 4.1c), the crest of the interface is pointier and at $1190 V_{pp}$ (Fig. 4.1d), it hits the wall and maintains that shape unless the applied voltage is increased. The voltage that causes the

interface to hit the wall is named as the hitting voltage. After increasing the applied voltage by around $200 V_{pp}$, micro droplets can be obtained. The shape of the interface doesn't change unless the voltage is increased.

The interface maintains the shape in Figure 4.1. d) unless the voltage is increased by around $200 V_{pp}$. The voltage increase below $200 V_{pp}$ does not affect the shape. After increasing the voltage above the hitting voltage by around $200 V_{pp}$, the continuous phase liquid starts to encapsulate the silicone oil as in Figure 4.2; therefore, silicone oil micro droplets in the shape of slugs are formed. The droplets can also be obtained by directly applying the electric field without gradually increasing from 0 V. The size of the droplets does not change with the method of applying the electric field.

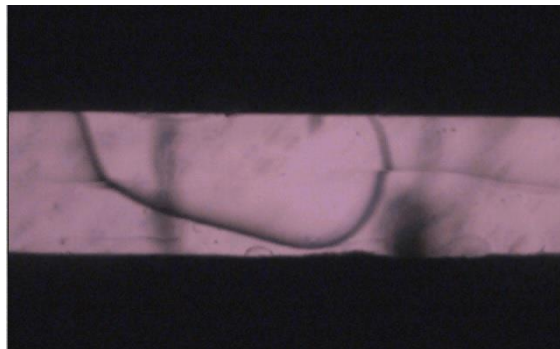


Figure 4.2. The first droplet formation for $100 \mu\text{L}/\text{min}$ and $200 \mu\text{L}/\text{min}$ for the silicone oil and 85% glycerol solution at $1400 V_{pp}$

4.1. Determining the Hitting Voltage

In the next section, the hitting voltage is investigated for the parameters, the thickness ratio, β , the total flow rate, TF, the function type of the AC electric field, and the rheology of the non-Newtonian liquid.

4.1.1. The Effect of the Thickness Ratio

In this section, the effect of the thickness ratio β , i.e. the ratio of the dispersed phase (oil) to the continuous phase (aqueous) to on the critical voltage is examined for various total flow rates which are 300 , 240 and $180 \mu\text{L}/\text{min}$. With the flow rate values below $180 \mu\text{L}/\text{min}$,

it is hard to obtain a stable interface. Since the minimum Reynolds Number is desired for microfluidics, the experiments are performed with the minimum flow rates possible. The highest worst case Reynold Number for our experiments would be with the 85% glycerol solution which has the highest viscosity. If we assume that only 85% glycerol solution is flowing in the channel with 300 $\mu\text{L}/\text{min}$, the calculated Reynolds Number would be 0.011.

4.1.1.1. The Effect of the Thickness Ratio for the Newtonian Liquid Couple. The interface position depends on the flow rate ratio. To see the dependence of the thickness ratio on the flow rate ratio, theoretical values are calculated by using the Navier-Stokes Equation as mentioned in Appendix A and experimental data are recorded. It is observed in the experiments that the interface position does not change with the total flow rate at the same flow rate ratios which is also valid for the theoretical results. Experimental and theoretical thickness ratio values are compared in Figure 4.3. and the error percentage is shown in Table 4.1. It is believed that the error is due to the 2D flow assumption. (Pohar et al., 2012)

In these experiments, silicone oil 10 cSt, and 85% glycerol solution are used as liquids. The AC electric field frequency was set to 5 kHz as default with sinusoidal wave form. The thickness ratio β , and the total flow rate parameters are investigated in Figure 4.4.

Table 4.1. Error analysis between the theoretical and experimental evaluation of the thickness ratios of the silicone oil 10 cSt to ethylene glycol as given in Figure 4.3.

Flow Rate Ratio	5.00	2.00	1.50	1.00	0.67
Thickness ratio (theo)	0.2244	0.4098	0.4851	0.6108	0.7516
Thickness ratio (exp)	0.1605	0.2857	0.3846	0.5000	0.6468
Error (%)	28.5	30.3	20.7	18.1	13.9

For the experiments performed with a total flow rate (TF) of 300 $\mu\text{L}/\text{min}$, flow rates are adjusted such that the β are 6.2, 3.5, 2.6 and 2.1. For the set with TF 240 $\mu\text{L}/\text{min}$, β are 3.5, 2.27, 2 and 1.4 and for the set with TF 180 $\mu\text{L}/\text{min}$, β are 3.5, 2.6, 2 and 1.4. Then the obtained data are compared in Figure 4.4. It is seen that as the thickness of the dispersed phase increases, the hitting voltage also increases. Therefore the system becomes more stable. The reason for this mechanism would be that it is related to the mass flow rate.

The effect of total flow rate TF, on the hitting voltage is also shown in Figure 4.4. The experiment set with the highest total flow rate, which is 300 $\mu\text{L}/\text{min}$, and it requires the highest hitting voltage. It is seen that the TF has definitely a stabilizing effect on the interface and since the difference between the hitting voltages of the different flow rates are not in each other's error bar, the change of the required hitting voltage is significant.

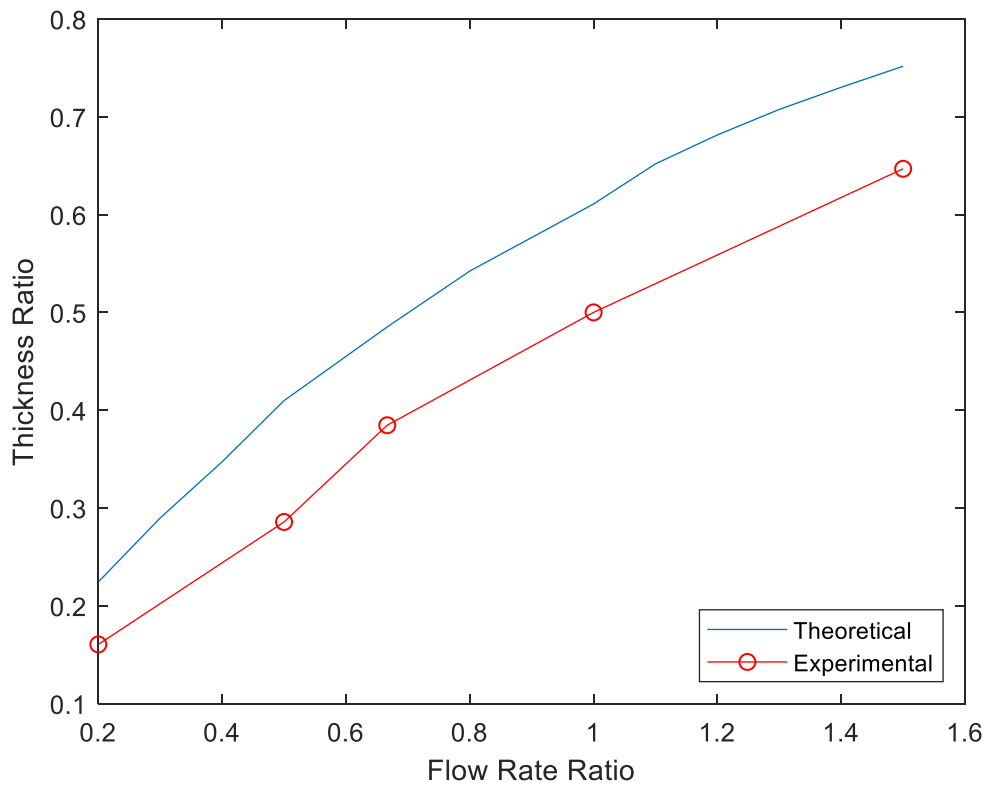


Figure 4.3. Theoretical and experimental thickness ratios comparison of the silicone oil 10 cSt and the 85% glycerol solution

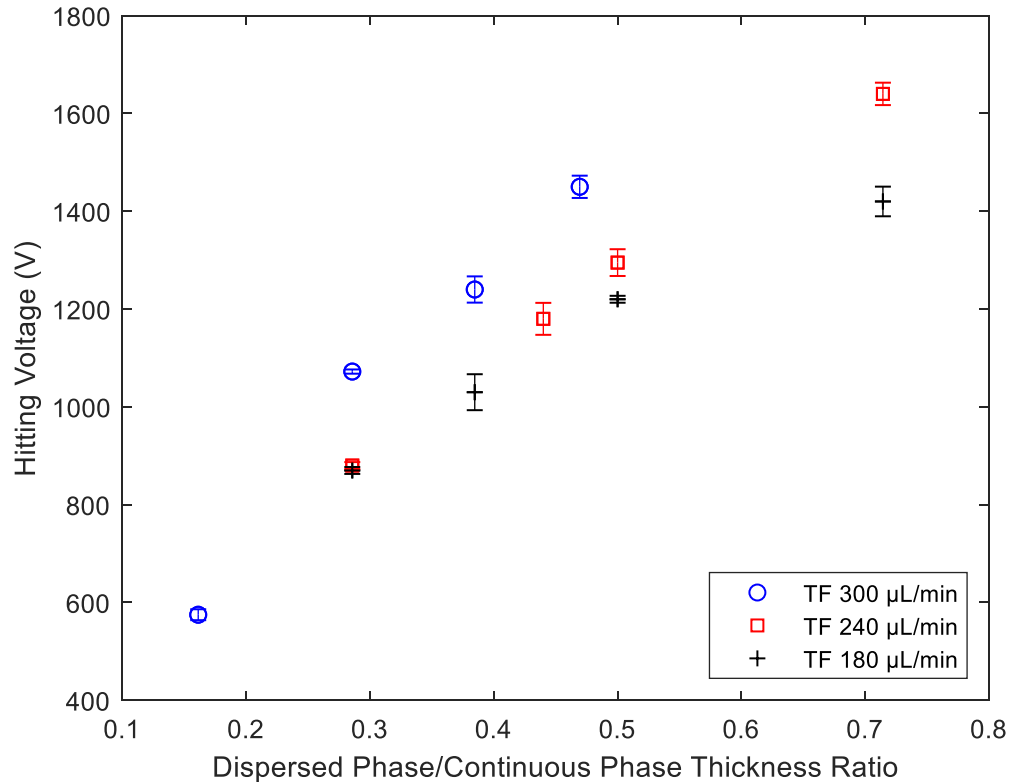


Figure 4.4. The hitting voltage of the Newtonian liquid couple for different thickness ratios and total flow rates of 300, 240, 180 $\mu\text{L}/\text{min}$ (TF).

4.1.1.2. The Effect of the Thickness Ratio for the Newtonian & non-Newtonian Couple. In Newtonian & non-Newtonian liquid couple experiments, silicone oil 10 cSt and 250 ppm xanthan gum in 85% glycerol solution were used. In Figure 4.5, the rheology of the non-Newtonian fluid is shown and it indicates that the liquid has a shear-thinning characteristic. AC electric field frequency was set to 5 kHz as default. The thickness ratio β and the total flow rate TF are the parameters studied and shown in Figure 4.6.

In the non-Newtonian experiments, the investigated TF is same as the Newtonian liquid couple as 300, 240 and 180 $\mu\text{L}/\text{min}$. The hitting voltages were observed for the thickness ratios β of 4.86, 3.82, 3.1 and 2.15 which are same for all TF. Similar to the Newtonian couple experiments, it is observed that the dispersed phase thickness has a stabilizing effect on the interface between the liquids. The increasing trend of the hitting voltage is different for the Newtonian & non-Newtonian couple. The Newtonian couple had

an exponential trend but for these experiments, the trend is linear. This means that for this liquid couple, β has a weaker effect on the stability of the interface.

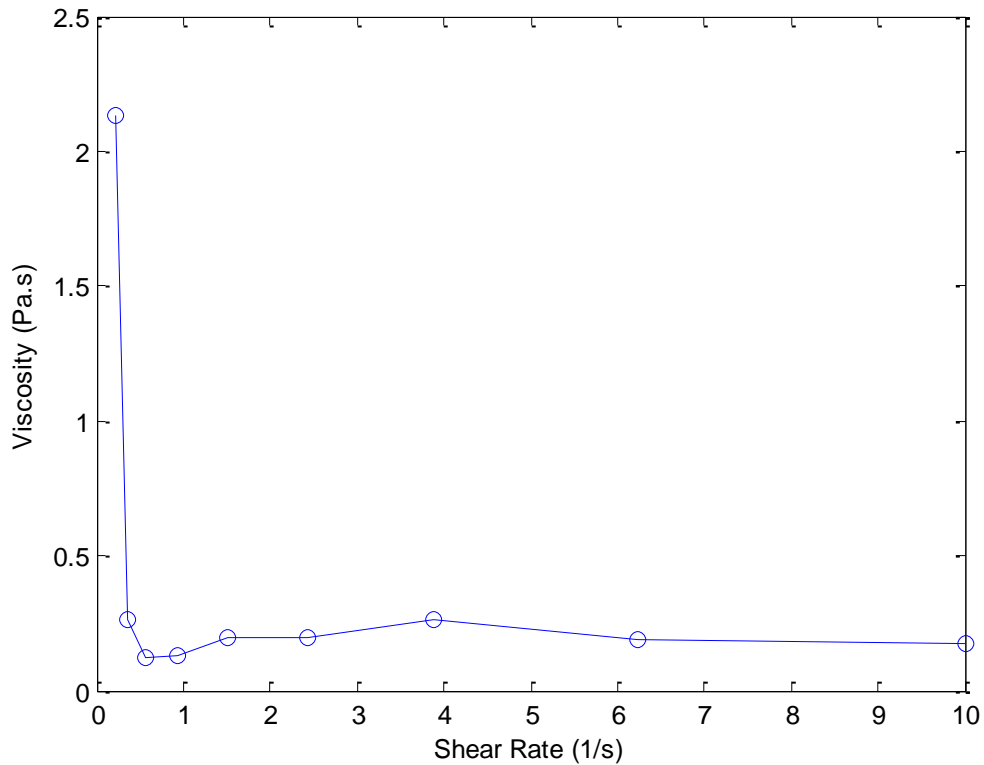


Figure 4.5. Rheology of 250 ppm 85% Glycerol Solution.

For the Newtonian & non-Newtonian liquid couple, the effect of TF is also shown in Figure 4.6. and the results show that, again similar to the Newtonian couple, the total flow rate has a stabilizing effect on the interface.

In Figure 4.7., the hitting voltage for the Newtonian and Newtonian & non-Newtonian couple are compared for a TF of 300 $\mu\text{L}/\text{min}$. The Newtonian & non-Newtonian couple has a more stable interface than the Newtonian couple. The reason for this difference in their behavior would be that, the additive increased the viscosity values of the liquid and provided more stable interface.

Table 4.2. Rheological data on the non-Newtonian liquid at 23°C.

Shear Rate (1/s)	Viscosity (Pa.s)
0.229	2.130
0.367	0.265
0.558	0.124
0.943	0.129
1.510	0.195
2.420	0.194
3.890	0.260
6.240	0.192
10.000	0.176

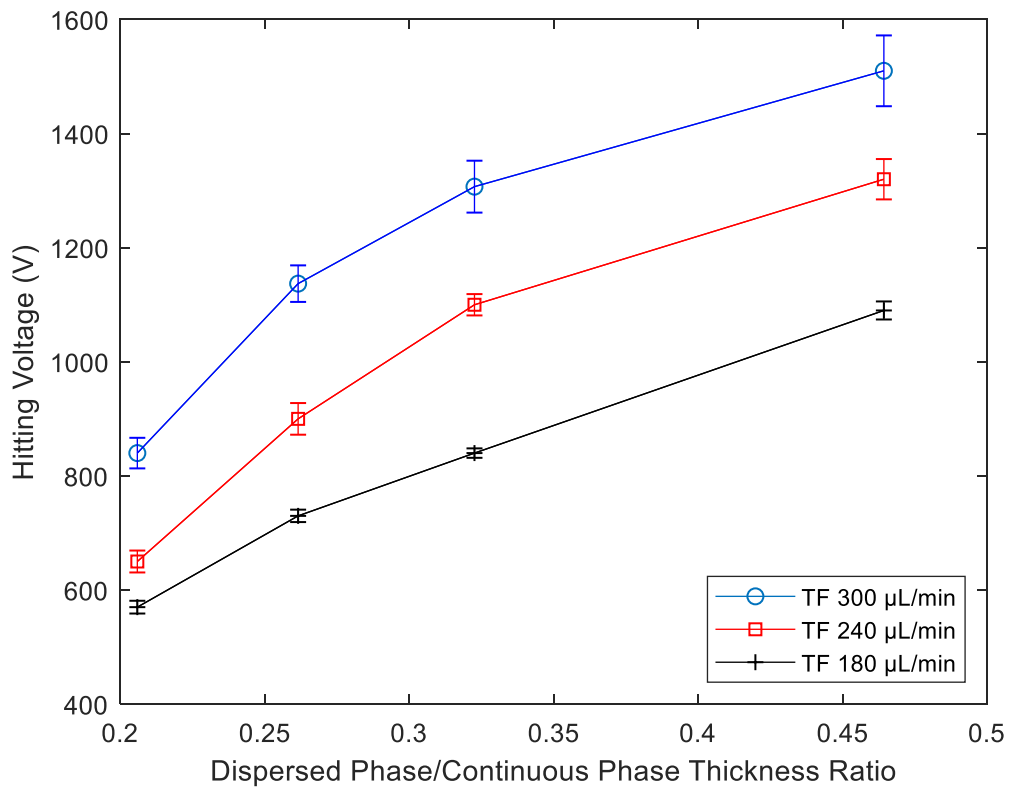


Figure 4.6. The hitting voltage of the Newtonian & non-Newtonian liquid couple for different thickness ratios and total flow rates of 300, 240, 180 $\mu\text{L}/\text{min}$.

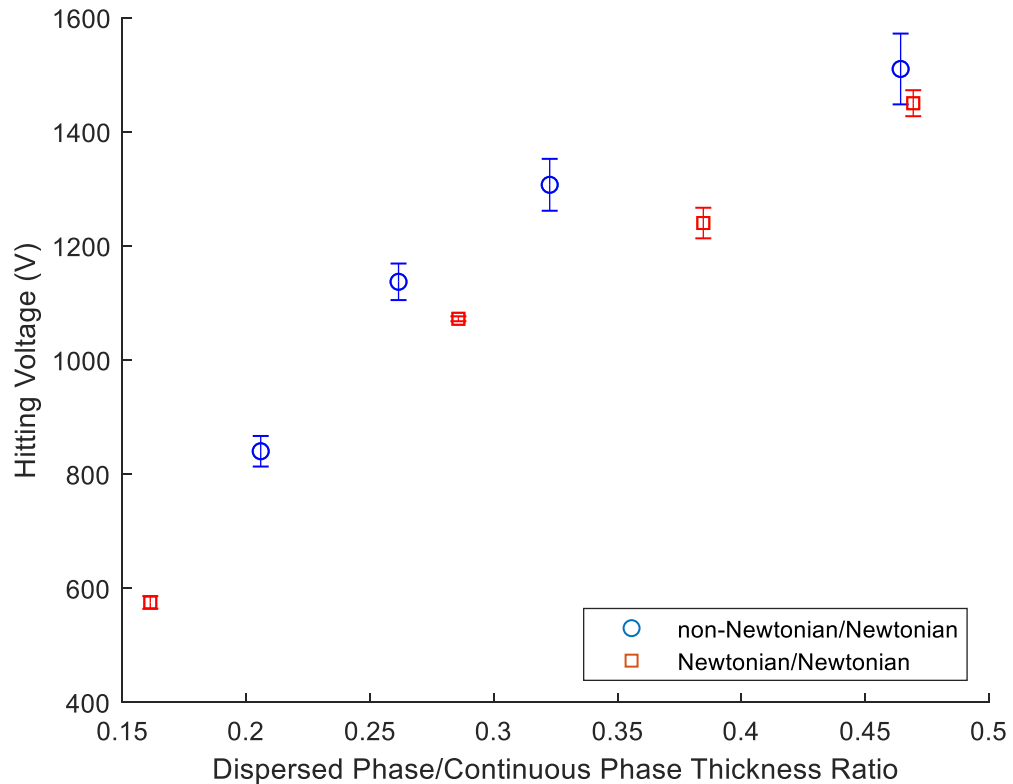


Figure 4.7. Comparison of the hitting voltage for the Newtonian and the Newtonian/non-Newtonian liquid couple at the flow rate of 300 $\mu\text{L}/\text{min}$.

4.1.2. The Effect of the AC Electric Field Wave Form

The function wave form of the AC electric field, i.e. sinusoidal or square, is studied in this section. The frequency of the waves are fixed to 5 kHz and total flow rate is 350 $\mu\text{L}/\text{min}$. Since the previous solution had water in composition, as dispersed and continuous phases, silicone oil 50 cSt and ethylene glycol are used. To prevent electrolysis for the continuous phase, 5 kHz frequency value is selected.

Figure 4.8 shows that the square function provides a lower hitting voltage than the sinusoidal function. It can be interpreted as the difference caused by the average of the applied voltage magnitude. For the square function, the average applied voltage magnitude equals to the maximum voltage magnitude. Different from the square function, for the sinusoidal function, the magnitude of the applied voltage changes periodically in time as

expressed by a sinusoidal curve. This, causes the average applied voltage to be lower than its maximum.

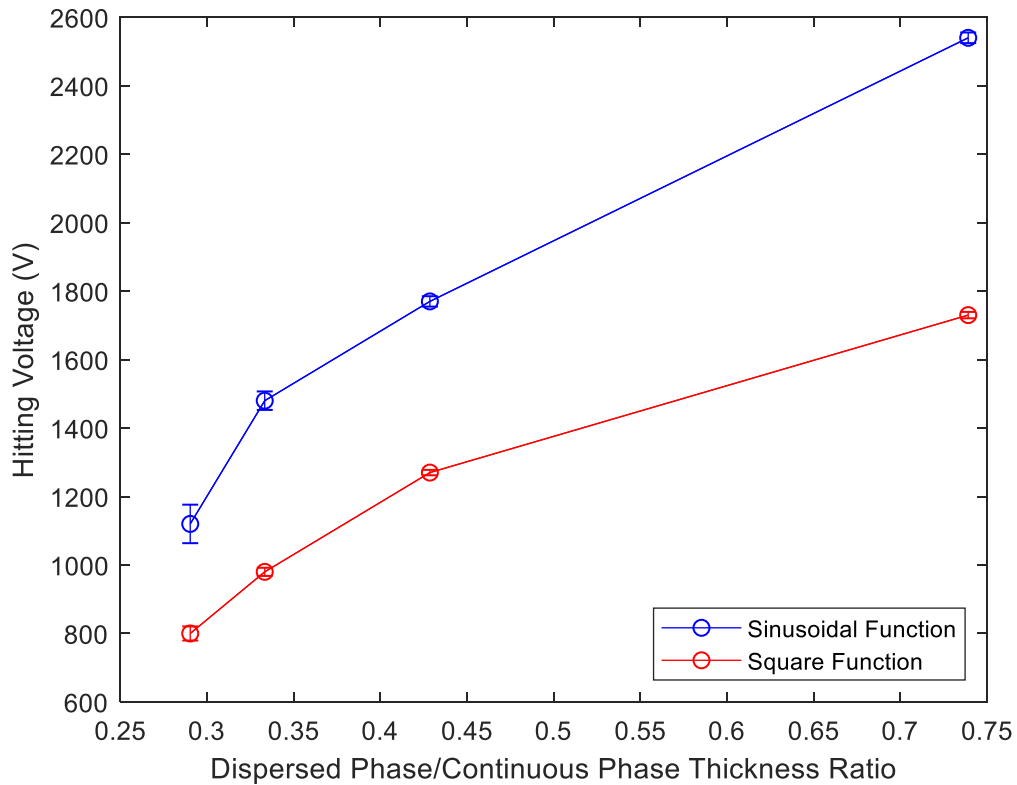


Figure 4.8. Comparison of the hitting voltages of the silicone oil 50 cSt and ethylene glycol liquid couple with the electric fields of sinusoidal and square waves at the total flow rate of 350 $\mu\text{L}/\text{min}$

4.1.3. The Effect of the Frequency of the AC Electric Field

Apart from the function type, another characteristic of the alternating current is the frequency of the wave. The effect of the frequency of the waves are investigated parametrically for both the square and the sinusoidal functions. The total flow rate is 350 $\mu\text{L}/\text{min}$ (50 $\mu\text{L}/\text{min}$ 50 cSt silicone oil and 300 $\mu\text{L}/\text{min}$ ethylene glycol) and the thickness ratio is selected as 0.43 for the experiments. Hitting voltages of the ethylene glycol and 50 cSt silicone oil couple are recorded for the frequencies in the range of 0.5 Hz to 40 kHz (Figure 4.9).

The frequency of the electric field has an interesting effect on the hitting voltage. Up to a specific frequency of 25 kHz, the hitting voltage has a constant value in both sinusoidal and square electric fields. No significant difference in the hitting voltage is observed. The peak for the required hitting voltage, occurred above 25 kHz and then it is constant again and increasing the frequency above 25 kHz does not increase the required hitting voltage Roberts and Kumar, (2009) have also determined theoretically through a Floquet analysis that the growth rate shows a jump at some certain frequencies depending on the system.

The hitting voltages of the square electric field are always lower than the sinusoidal field (Figure 4.9). Even the higher hitting voltage value of the square electric field (above 25 kHz) is smaller than the lower hitting voltage of the sinusoidal electric field (below 25 kHz).

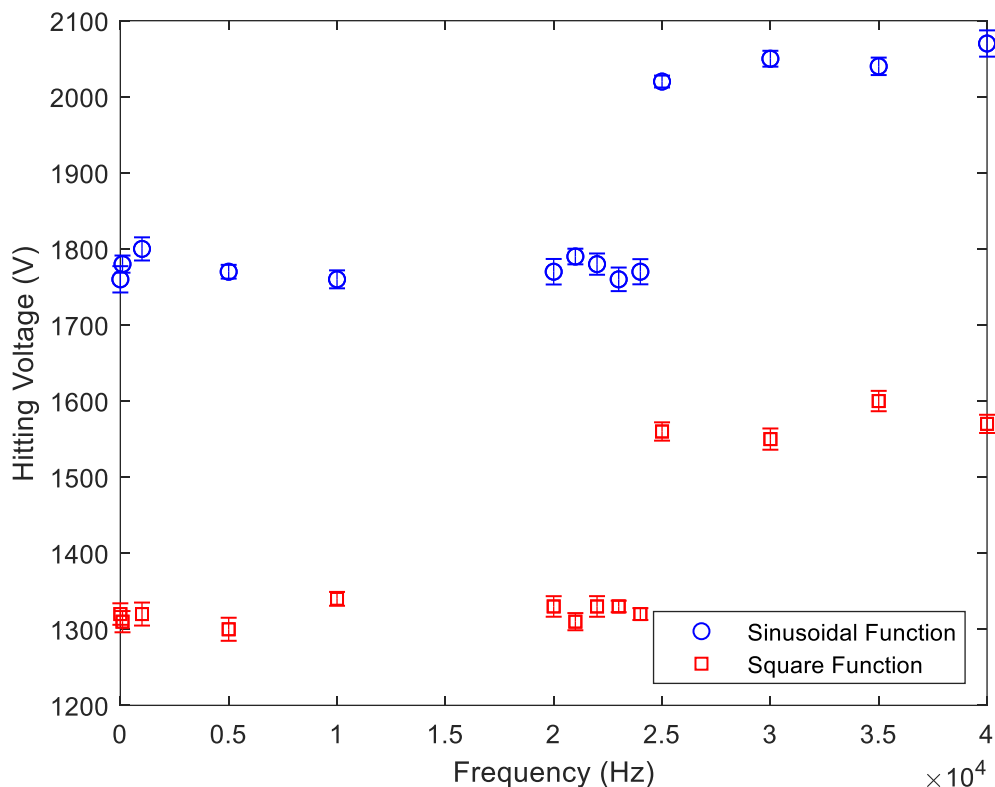


Figure 4.9. Frequency dependency of the hitting voltage at the sinusoidal and square electric field with the silicone oil 10 cSt and ethylene glycol liquid couple at the total flow rate of 350 $\mu\text{L}/\text{min}$

4.2.1. Applications

It is managed to perform some applications of droplets, which are particle encapsulation and ability to generate different sized droplets without changing the flow rates, frequency or applied voltage. These performed experiments can only be reproduced with the same flow rates, frequencies and channel.

4.2.1. Particle Encapsulation

It is investigated whether it is possible to encapsulate micro particles in micro droplets that are formed in a microchannel by using an electric field. The same channel with the liquid couple of ethylene glycol and spherical polyethylene particles with 150-180 μm diameter mixed with 50 cSt silicon oil are used for these experiments. In the experiments, 2500 V_{pp} electric field that has a sinusoidal wave form is applied directly without increasing the voltage gradually.

The experiments are performed with a total flow rate of 70 $\mu\text{L}/\text{min}$. The flow rate is significantly smaller than the other experiments to have a better control on the particle flow. With higher flow rates, it is harder to see and catch the particles. Ethylene glycol and 50 cSt silicone oil flow rates are 20 and 50 $\mu\text{L}/\text{min}$, respectively.

It is demonstrated that encapsulating particles is possible. But doing it in a controlled manner requires a deeper research. The particles cannot be sent to the microchannel homogenously. Sometimes they come as one at once and sometimes five of them are together. If this problem can be solved in further research, it will be possible to encapsulate them in a controlled way.

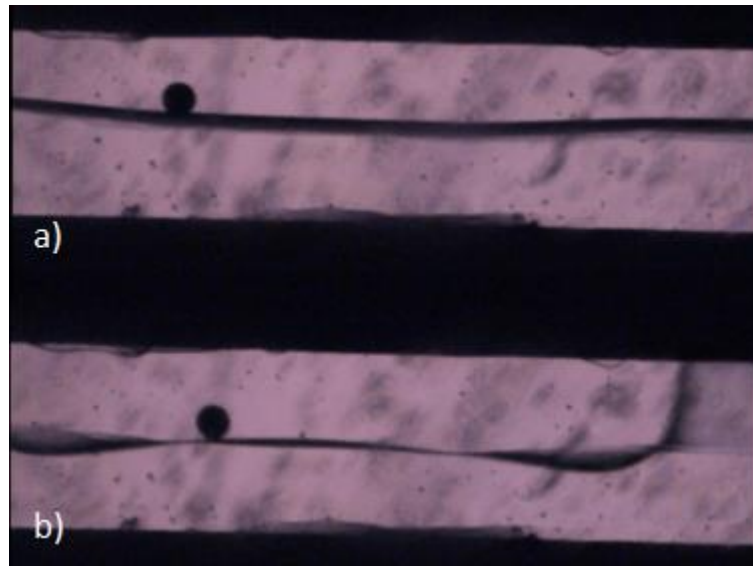


Figure 4.10. Initial interface deflection at particle encapsulation experiments with the flow rates of $20 \mu\text{L}/\text{min}$ 50 cSt silicone oil and $50 \mu\text{L}/\text{min}$ ethylene glycol a) Particle at stable interface at the silicone oil side b) First hit of the interface to the wall at $2500 V_{pp}$

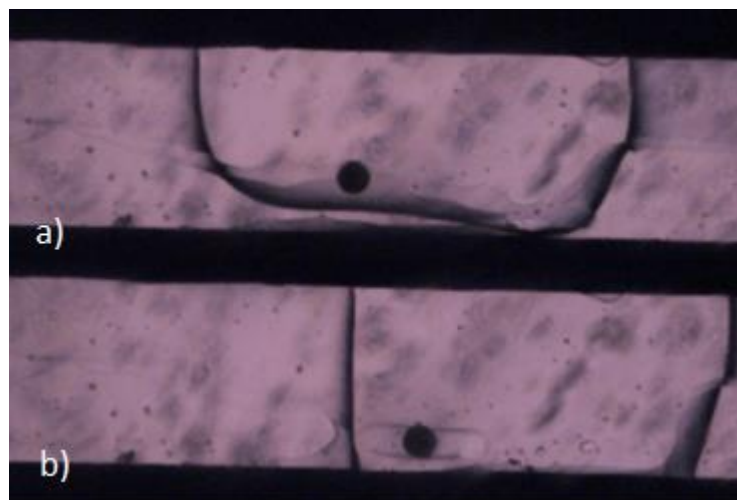


Figure 4.11. Particle encapsulation with the flow rates of $50 \mu\text{L}/\text{min}$ 50 cSt silicone oil and $20 \mu\text{L}/\text{min}$ ethylene glycol a) First encapsulation in $2500 V_{pp}$ b) The slug form after the first encapsulation

4.2.2. Generating Two Droplets with Different Sizes

At frequencies smaller than 2 Hz, periodical behavior of the interface is observed. When a voltage above the hitting voltage is directly applied with a frequency below 2 Hz, even though the voltage value is not changed from the function generator, the real applied voltage changes with time. This voltage change is caused from the ups and downs of the sinusoidal wave. With this behavior, droplets with different sizes can be generated. When sinusoidal wave climbs, first it reaches the hitting voltage and then it goes to the peak of the sinusoidal wave. At that point, a small droplet is generated. After the peak point as the voltage follows the sinusoidal wave, it's value decreases. Therefore a big droplet is generated. When it reaches 0 V_{pp} , it stabilizes again. this behavior is shown in Figure 4.13.

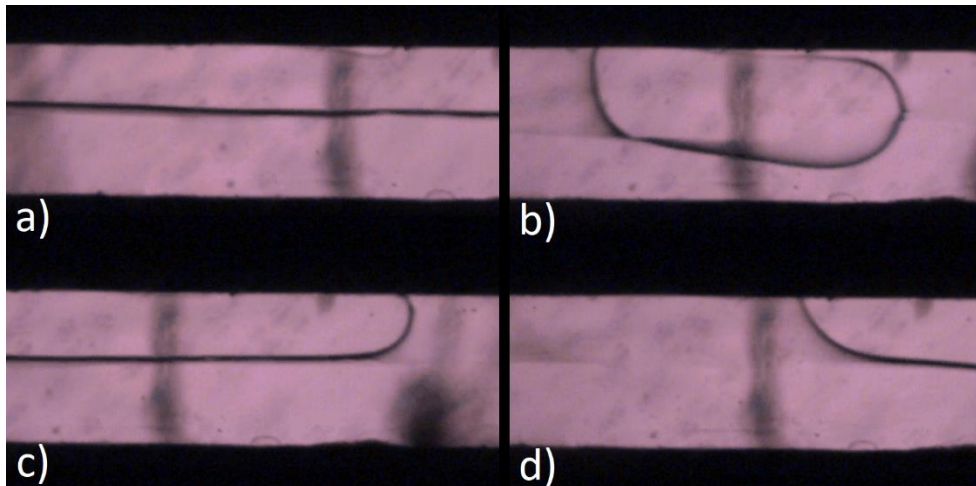


Figure 4.12 Droplet generation with the flow rates of 100 $\mu\text{L}/\text{min}$ 50 cSt silicone oil and 500 $\mu\text{L}/\text{min}$ ethylene glycol a) Stable interface b) Small droplet generated with directly applied 1300 V_{pp} at 0.33 Hz c) Big droplet's head d) Big droplet's back

5. CONCLUSION

The electrohydrodynamic instability between Newtonian/Newtonian and Newtonian/non-Newtonian liquid couples flowing in a microchannel is experimentally studied. The AC electric field is applied normal to the interface between the immiscible liquids. The hitting voltage is determined as a function of frequency, thickness ratio of the liquids, sinusoidal and square function effect. Additionally, particle encapsulation experiments are performed.

First, the thickness ratio of the liquids, β is studied for the Newtonian/Newtonian case, i.e., silicone oil 50 cSt and ethylene glycol. It is seen that increasing β , the thickness ratio has an increasing effect on the hitting voltage. For the Newtonian/non-Newtonian case, silicone oil 10 cSt and 250 ppm xanthan gum %85 glycerol solution are used. For this case, the β had also an increasing effect. The total flow rate increases the hitting voltage for both liquid couples but the effect is more significant for the Newtonian/non-Newtonian liquid couple.

The frequency effect on the hitting voltage for the Newtonian/Newtonian couple is analyzed. Up to the certain frequency value of 25 kHz, the hitting voltage does not change. But then, the hitting voltage makes a jump. After making the jump, increasing the frequency further does not change the hitting voltage.

The AC field is also applied with square function to compare to the default function, which is sinusoidal. Experiments are performed with the Newtonian/Newtonian couple. The square function provided lower hitting voltages and also increasing the hitting voltage trend with the thickness ratio is linear similar to the Newtonian/non-Newtonian case.

Particle encapsulation experiments showed that encapsulating particles with a droplet can be achieved, but a better controlled and more robust experimentation is needed. And with the frequencies below 2 Hz, with the same applied voltage, different sized droplets can be generated due to the sinusoidal wave ups and downs.

REFERENCES

- Anna, S.L., N. Bontoux, and H. A. Stone, 2003, "Formation of Dispersions Using Flowfocusing in Microchannels", *Applied Physics Letters*, Vol. 82, No. 3, pp. 364-366.
- Anthony Anthonsamy, Raymond. (2007). *Designing, Fabricating And Characterizing A Microfluidic Capacitor*.
- Castro-Hernández, E., García-Sánchez, P., Velencoso-Gómez, A., Silas-Jurado, A., Fernandez Rivas, D., & Ramos, A., 2017, "Droplet group production in an AC electro-flow-focusing microdevice", *Microfluidics and nanofluidics*, Vol. 21, No. 5.
- Chen, C. T. and Lee G. B., 2006, "Formation of Microdroplets in Liquids Utilizing Active Pneumatic Choppers on a Microfluidic Chip", *Journal of Microelectromechanical Systems*, Vol. 15, No. 6, pp. 1492-1498.
- de Mello, A. J., 2001, "DNA Amplification: Does Small Really Mean Efficient?", *Lab on a Chip*, Vol. 1, pp. 24-29.
- Haiwang, Li & Teck Neng, Wong & Nguyen, Nam-Trung. (2012). Electrohydrodynamic and Shear-Stress Interfacial Instability of Two Streaming Viscous Liquid Inside a Microchannel for Tangential Electric Fields. *Micro and Nanosystems*. 4. 14-24. 10.1115/ICNMM2011-58089.
- Hatakeyema, T., D. L. L. Chen, R. F. Ismagilov, 2006, "Microgram-Scale Testing of Reaction Conditions in Solution Using Nanoliter Plugs in Microfluidics with Detection by MALDI-MS", *Journal of the American Chemical Society*, Vol. 128, pp. 2518-2519.
- Huang, Y., Y. L. Wanga and T. N. Wong, 2017, "AC electric field controlled non-Newtonian filament thinning and droplet formation on the microscale", *Lap on a Chip*, Vol. 17, pp. 2969-2981

- Kunti, Golak & Bhattacharya, Anandaroop & Chakraborty, Suman. (2017). Analysis of micromixing of non-Newtonian fluids driven by alternating current electrothermal flow. *Journal of Non-Newtonian Fluid Mechanics*, 247. Vol. 10.1016/j.jnnfm.2017.06.010.
- Li, Di & Xuan, Xiangchun. (2018). Fluid rheological effects on particle migration in a straight rectangular microchannel. *Microfluidics and Nanofluidics*, Vol. 22. 10.1007/s10404-018-2070-4.
- Li, F., O. Ozen, N. Aubry, D. T. Papageorgiou, and P. G. Petropoulos, 2007, “Linear Stability of a Two-Fluid Interface for Electrohydrodynamic Mixing in a Channel”, *Journal of Fluid Mechanics*, Vol. 583, pp. 347–377.
- Li, H., T. N. Wong, N. T. Nguyen, 2012, “Instability of Two Pressure Driven Viscous Fluid Streams in a Microchannel Under a Normal Electric Field”, *International Journal of Heat and Mass Transfer*, Vol. 55, No. 2324, pp. 6994-7004
- Melcher, J. R., and C. V. Smith, 1969, “Electrohydrodynamic Charge Relaxation Overstability and Interfacial Perpendicular Field Instability”, *Physics of Fluids*, Vol. 12, pp. 778-790.
- Melcher, J.R. and W. J. Schwarz, 1968, “Interfacial Relaxation Overstability in a Tangential Electric-Field”, *Physics of Fluids*, Vol. 11, pp. 2604-2616.
- Murshed, S. M. S., N. T. Nguyen, and S. H. Tan, 2008a, “Temperature Dependence of Interfacial Properties and Viscosity of Nanofluids for Droplet-Based Microfluidics”, *Journal of Physics D: Applied Physics*, Vol. 41, No. 8.
- Murshed, S. M. S., N. T. Nguyen, S. H. Tan, T. N. Wong, and Yobas, L., 2008b, “Thermally Controlled Droplet Formation in Flow Focusing Geometry: Formation Regimes and Effect of Nanoparticle Suspension”, *Journal of Physics D: Applied Physics* Vol. 41, No. 16.

- Nam, J., H. Lim, D. Kim, H. Jungb and S. Shin, "Continuous separation of microparticles in a microfluidic channel via the elasto-inertial effect of non-Newtonian fluid", *Lab Chip*, 12, 1347 (2012)
- Nguyen, N. T., T. H. Ting, Y. F. Yap, T. N. Wang, J. C. K. Chai, W. L. Ong, J. Zhou, S. H. Tang, and L. Yobaş, 2007, "Thermally Mediated Droplet Formation in Microchannels", *Applied Physics Letters*, Vol. 91, pp. 084102.1-084102.3
- Ozen O., N. Aubry, D. T. Papageorgiou, and P. G. Petropoulos, 2006a, "Monodisperse drop Formation in Square Microchannels", *Physics Review Letters*, Vol 96, No. 14.
- Ozen, O., D. T. Papageorgiou, and P. G. Petropoulos, 2006b, "Nonlinear Stability of a Charged Electrified Viscous Liquid Sheet under the Action of a Horizontal Electric Field", *Physics of Fluids*, Vol. 18, No. 042102.
- Ozen, O., N. Aubry, D. Papageorgiou, and P. Petropoulos, 2006c, "Electrohydrodynamic Linear Stability of Two Immiscible Fluid in Channel Flow", *Electrochimica Acta*, Vol. 51, pp. 5316-5323.
- Pohar, A., Lakner, M., Plazl, I., 2012, "Parallel flow of immiscible liquids in a microreactor: modeling and experimental study", *Microfluid Nanofluid* 12, pp. 307-316,
- Raj M., Bhattacharya, S., DasGupta, S., Chakraborty, S., 2018, Collective dynamics of red blood cells on an in vitro microfluidic platform, *Lab on a Chip*, Vol. 18, 3939-3948
- Ren, Q., 2018, Investigation of pumping mechanism for non-Newtonian blood flow with AC electrothermal forces in a microchannel by hybrid boundary element method and immersed boundary-lattice Boltzmann method. *Electrophoresis*, Vol. 39. 10.1002/elps.201700494.

- Roberts, S. A. and S. Kumar, 2009, "AC Electrohydrodynamic Instabilities in Thin Liquid Films", *Journal of Fluid Mechanics*, Vol. 631, pp. 255-279.
- Roumpea, E., & M. Chinaud, and P. Angeli., 2017. Experimental Investigations of Non-Newtonian/Newtonian Liquid-Liquid Flows in Microchannels. *AIChE Journal*, Vol. 63. 10.1002/aic.15704.
- Ezazi Sarang, Hadjiaghayie Vafaie Reza, 2017, "Generating efficient chaos effect in micro channel using electrohydrodynamic theory", Vol. 55, pp. 745-753
- Schäffer, E., T. Thurn-Albrecht, T. P. Russell, and U. Steiner, 2001, "Electrohydrodynamic Instabilities in Polymer Films", *Europhysics Letters*, Vol. 53, No. 4, pp. 518–523
- Sharma, Sanjiv & Srisa-Art, Monpichar & Scott, Steven & Asthana, Amit & Cass, Tony. (2013). *Droplet-Based Microfluidics. Methods in molecular biology* (Clifton, N.J.). 949. 207-230. 10.1007/978-1-62703-134-9_15.
- Song, H., D. L. Chen, and R. F. Ismagilov, 2006, "Reactions in Droplets in Microfluidic Channel", *Angewandte Chemie International Edition*, Vol. 45, No. 44, pp. 7336-7356.
- Song, H. and R. F. Ismagilov, 2003, "Milisecond Kinetics on a Microfluidic Chip Using Nanoliters of Reagents", *Journal of the American Chemical Society*, Vol. 125, pp. 14613-14619.
- Soni, P., R. M. Thakkar, and V. A. Juvekar, 2018, "Electrohydrodynamics of a concentric compound drop in an AC electric field", Vol. 30, No. 32102
- Tan S. H., N. T. Nguyen, L. Yobaş, and T. G. Kang, 2010, "Formation and Manipulation of Ferrofluid Droplets at a Microfluidic T-Junction", *Journal of Micromechanics and Microengineering*, Vol. 20, No. 4, No. 045004.

- Tan, S. H., S. M. Murshed, N. T. Nguyen, T. N. Wong, and L. Yobas, 2008, "Thermally Controlled Droplet Formation in Flow Focusing Geometry: Formation Regimes and Effect of Nanoparticle Suspension", *Journal of Physics D: Applied Physics*, Vol. 41, No. 165501.
- Tan, Y. C. and Lee, A. P., 2005, "Microfluidic Separation of Satellite Droplets as the Basis of a Monodispersed Micron and Submicron Emulsification System", *Lab on a Chip*, Vol. 6, pp. 1178-1183.
- Thorsen, T., R. W. Roberts, F. H. Arnold, S. R. Quake, 2001, "Dynamic Pattern Formation in a Viscle-Generating Microfluidic Device", *Physical Review Letters*, Vol. 86, No. 18, pp. 4163-4166.
- Uguz, A. K., and N. Aubry, 2008, "Quantifying the Linear Stability of a Flowing Electrified Two-Fluid Layer in a Channel for Fast Electric Times for Normal and Parallel Electric Fields", *Physics of Fluids*, Vol. 20, No. 092103.
- Uguz, A. K., O. Ozen, and N. Aubry, 2008, "Electric Field Effect on a Two-Fluid Interface Instability in Channel Flow for Fast Electric Times", *Physics of Fluids*, Vol. 20, No. 031702.
- Umbanhowar, P.B., V. Prasad, D. A. Weitz, 2000, "Monodisperse Emulsion Generation via Drop Break Off in a Co-flowing Stream", *Langmuir*, Vol. 16, No. 2, pp. 347-351.
- Willaime, H., V. Barbier, L. Kloul, S. Maine, and P. Tabeling, 2006, "Arnold Tongues in a Microfluidic Drop Emitter", *Physical Review Letters*, Vol. 96, No. 054501.
- Wang Q, Papageorgiou DT. (2018) Using electric fields to induce patterning in leaky dielectric fluids in a rod-annular geometry. *IMA J. Appl. Math.* 83:24–52
- Wong, Voon Loong & Loizou, Katerina & Lau, Phei-Li & Graham, Richard & Hewakandamby, Buddhika. (2014). Numerical Simulation of the Effect of Rheological Parameters on Shear-Thinning Droplet Formation. *American Society of*

Mechanical Engineers, Fluids Engineering Division (Publication) FEDS, Vol. 2, 10.1115/FEDSM2014-21363.

Zheng, B., J. D. Tice, R. F. Ismagilov, 2004, "Formation of Droplets of Alternating Composition in Microfluidic Channels and Applications to Indexing of Concentrations in Droplet-Based Assays", *Analytical Chemistry*, Vol. 76, pp. 4977-4982.

Zhu, Pingan & Wang, Liqiu. (2016). Passive and active droplet generation with microfluidics: a review. *Lab Chip*. 17. 34-75. 10.1039/C6LC01018K.

APPENDIX A: INTERFACE POSITION

As mentioned in Section 4.1.1.1., the experimental interface position is compared with theoretical interface position. For this reason, the theoretical interface position is found in this section. The physical system is depicted in Figure A1 where the fluids flow side by side

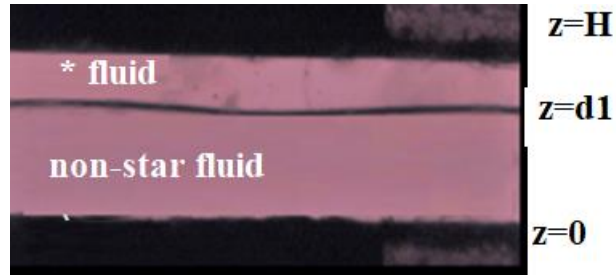


Figure A.1. Physical system of the microchannel

The Navier-Stokes equations are simplified when the flow is laminar. The laminar velocity profiles are found by simplifying the Navier-Stokes equations as

$$\mu^* u_{zz}^* = P_x \quad (\text{A.1})$$

and

$$\mu u_{zz} = P_x \quad (\text{A.2})$$

for both phases. Here, u is the x-component of the velocity and P_x is the pressure gradient which is constant. The * fluid is the top and the non-star fluid is the bottom fluid. After that the velocity profiles are found by integrating these equations. The velocity profiles are found as

$$u^* = \alpha_1 z^2 + c_{11} z + c_{12} \quad (\text{A.3})$$

$$u = \alpha_2 z^2 + c_{21} z + c_{22} \quad (\text{A.4})$$

The unknown four constants are found from the no-slip boundary conditions on the walls (located at $z = 0$ and $z = d_1 + d_2 = H$) and at the interface (located at $z = d_1$) and the continuity of the stress at the interface given as

$$u^*(H) = 0 \quad (\text{A.5})$$

$$u(0) = 0 \quad (\text{A.6})$$

$$u(d_1) = u^*(d_1) \quad (\text{A.7})$$

and

$$\mu u_z(d_1) = \mu^* u_{zz}^* \quad (\text{A.8})$$

respectively. At this point, the constant can be found from the boundary and the interface positions. Thus, the pressure gradient and the interface position are unknown. The individual flow rates of fluids can be determined by integrating the velocities over the cross sectional areas and the volumetric flow rates are known in the experiments. The integrals are

$$Q^{(1)} = D \int_{d_2}^{d_1+d_2} u^* dz \quad (\text{A.9})$$

$$Q^{(2)} = D \int_0^{d_1} u dz \quad (\text{A.10})$$

where D is the uniform channel depth. The position of the interface is determined in Matlab as a function of viscosity and volumetric flow rate ratios.